

Dependent Dirichlet processes via thinning

Laura D'Angelo, and Bernardo Nipoti, and Andrea Ongaro
University of Milano-Bicocca, Italy

Abstract

When analyzing data from multiple sources, it is often convenient to strike a careful balance between two goals: capturing the heterogeneity of the samples and sharing information across them. We introduce a novel framework to model a collection of samples using dependent Dirichlet processes constructed through a thinning mechanism. The proposed approach modifies the stick-breaking representation of the Dirichlet process by thinning, that is, setting equal to zero a random subset of the beta random variables used in the original construction. This results in a collection of dependent random distributions that exhibit both shared and unique atoms, with the shared ones assigned distinct weights in each distribution. The generality of the construction allows expressing a wide variety of dependence structures among the elements of the generated random vectors. Moreover, its simplicity facilitates the characterization of several theoretical properties and the derivation of efficient computational methods for posterior inference. A simulation study illustrates how a modeling approach based on the proposed process reduces uncertainty in group-specific inferences while preventing excessive borrowing of information when the data indicate it is unnecessary. This added flexibility improves the accuracy of posterior inference, outperforming related state-of-the-art models. An application to the Collaborative Perinatal Project data highlights the model's capability to estimate group-specific densities and uncover a meaningful partition of the observations, both within and across samples, providing valuable insights into the underlying data structure.

Keywords: Dependent Dirichlet process; Model-based clustering; Partially exchangeable data; Stick-breaking prior; Thinning.

1 Introduction

Over the past 25 years, considerable attention has been dedicated to the study of dependent nonparametric priors for collections of random probability measures indexed by a covariate. A recent review by [Quintana et al. \(2022\)](#) highlights many key contributions in this area. [Franzolini et al. \(2025\)](#) introduce a unifying framework that clarifies how these contributions fit within the broader class of multivariate species sampling models. A general distribution theory of hierarchical processes is presented in [Camerlenghi et al. \(2019\)](#). The dependent Dirichlet process (DDP), introduced by [MacEachern \(2000\)](#) in a seminal paper, remains arguably the most popular prior of this type. The DDP extends the use of the Dirichlet process (DP) to nonparametric regression, enabling the modeling of the conditional distribution of the response given some covariate. The definition of the DDP builds on the stick-breaking representation of the DP, as introduced in [Sethuraman \(1994\)](#). This constructive definition characterizes a random distribution p on a measurable space (Θ, \mathcal{B}) starting from two sequences of independent and identically distributed (iid) random variables $\{v_j\}_{j \geq 1}$ and $\{\theta_j\}_{j \geq 1}$, independent of each other. Assuming $v_j \stackrel{\text{iid}}{\sim} \text{Beta}(1, \alpha)$ with $\alpha > 0$, and $\theta_j \stackrel{\text{iid}}{\sim} P_0$, where P_0 is a probability distribution on (Θ, \mathcal{B}) , for $j \geq 1$, [Sethuraman \(1994\)](#) showed that a DP with base measure P_0 and total mass α can be expressed as

$$p(\cdot) = \sum_{j=1}^{\infty} \omega_j \delta_{\theta_j}(\cdot), \quad (1)$$

where δ_{θ_j} indicates a Dirac mass at the location θ_j , and the probabilities are defined as $\omega_1 = v_1$, $\omega_j = v_j \prod_{h < j} (1 - v_h)$ for $j > 1$. The DDP extends this formulation by defining a collection of random probability measures p_x , indexed by a covariate $x \in \mathcal{X}$, through modifications to the stick-breaking representation of the DP. Specifically, either the weights, the atoms, or both are replaced with stochastic processes indexed by x . This construction preserves the desirable property that the marginal distribution at each covariate value remains a DP. Moreover, when the covariate indexing the collection of random probability measures is categorical, say g with levels $\{1, \dots, G\}$, case considered throughout this work,

the DDP serves as a convenient prior modeling data structured into distinct yet related groups, e.g. patients undergoing different treatments. A notable instance of MacEachern’s DDP is the single-atom DDP. As the name suggests, this specification maintains a common set of atoms across all covariate values, introducing dependence solely through the weights. This formulation has been widely studied, particularly for modeling dependence over time (Griffin & Steel 2011) and across spatial locations (Duan et al. 2007, Fuentes & Reich 2013). A related approach was proposed by Griffin & Steel (2006), with the dependence between DPs introduced by modifying the ordering of the Beta-distributed random variables in their stick-breaking construction. Models for dependent probability measures based on the idea of sharing some or all the atoms extend beyond the DDP framework. The hierarchical Dirichlet process (HDP, Teh et al. 2006) models a collection of probability distributions as distinct DPs, introducing dependence and shared atoms by modeling the common base measure as a DP itself. The common atoms model (CAM, Denti et al. 2023) employs a nested DP structure with a shared set of atoms to jointly cluster groups defined by covariate values and individual observations. The Griffiths-Milne dependent Dirichlet process (GM-DDP, Lijoi et al. 2014) takes a different approach that explicitly distinguishes between covariate-specific and shared atoms, by defining a vector of dependent DPs as the superposition of covariate-specific processes and a shared one.

We introduce the thinned dependent Dirichlet process (thinned-DDP), a novel nonparametric prior for modeling collections of dependent random probability measures (p_1, \dots, p_G) . This prior is derived by thinning the atoms of a common DP. Instead of directly selecting the atoms θ_j that contribute to the definition of a covariate-specific random probability measure p_g , the approach we propose modifies the common weights ω_j in (1) by multiplying the common random variables v_j by covariate-specific thinning variables $\ell_{j,g} \in \{0, 1\}$, which determine whether the corresponding atoms θ_j appear in the definition of p_g . This approach retains the simplicity and tractability of the original stick-breaking construc-

tion, enabling analytical study of the properties of the thinned-DDP, and facilitating the adaptation of computational methods originally developed for a single DP to multi-sample settings. Unlike the single-atom DDP, the HDP, and the CAM, where all atoms are shared by all distributions, the thinned-DDP allows atoms to be either shared among subsets of measures or specific to individual ones. Moreover, the thinned-DDP offers a more flexible dependence structure compared to the GM-DDP. While both approaches account for the presence of shared and non-shared atoms, the thinned-DDP, unlike the GM-DDP, allows atoms to be shared by specific subsets of covariate-specific processes rather than by all of them. Finally, we observe that the idea of tilting the definition of a nonparametric process via thinning, that is by skipping some of its atoms, has found application in some recent contributions: [Lau & Cripps \(2022\)](#) introduced thinned completely random measures to model dependent hazard functions; the quasi-Bernoulli stick-breaking process of [Zeng et al. \(2023\)](#) uses a related idea to improve estimation of the number of clusters; [Bi & Ji \(2024\)](#) applied a thinning mechanism to the HDP to explicitly identify which atoms are specific to populations or common across them.

The remainder of this work is organized as follows. Section 2 introduces the thinned-DDP and explores its prior properties. A notable instance of the thinned-DDP, named eventually single-atom thinned-DDP, is presented in Section 2.1. Section 3 discusses two prior specifications for the sequences of thinning variables and what these imply for the resulting process. In Section 4, we define a mixture model with thinned-DDP-distributed mixing measures and outline a blocked Gibbs sampler for posterior inference. Section 5 presents a simulation study, including comparisons with state-of-the-art models. In Section 6, we apply the proposed model to a real dataset on the gestational age of women from different hospitals. Proofs and additional results are available as Supplementary Material.

2 Dependent Dirichlet processes via thinning

We let g be a categorical covariate with a finite number of levels, say $\{1, \dots, G\}$. In addition to the components underlying the stick-breaking construction of a DP given in (1), namely $v_j \stackrel{\text{iid}}{\sim} \text{Beta}(1, \alpha)$ with $\alpha > 0$ and $\theta_j \stackrel{\text{iid}}{\sim} P_0$ for $j \geq 1$, we introduce G sequences of thinning variables $\{\ell_{j,g}\}_{j \geq 1}$, for $g = 1, \dots, G$, where $\ell_{j,g} \in \{0, 1\}$ and $\sum_{j=1}^{\infty} \ell_{j,g} = \infty$. We let $\ell_{1:G}$ denote the collection of these sequences. For each realization of the covariate $g \in \{1, \dots, G\}$, we define a random probability measure p_g on (Θ, \mathcal{B}) as

$$p_g(\cdot) = \sum_{j=1}^{\infty} \omega_{j,g} \delta_{\theta_j}(\cdot) = \sum_{j=1}^{\infty} \left[v_j \ell_{j,g} \prod_{h < j} (1 - v_h \ell_{h,g}) \right] \delta_{\theta_j}(\cdot). \quad (2)$$

Definition 1. A thinned dependent Dirichlet process with concentration parameter $\alpha > 0$, base probability measure P_0 , and thinning sequences $\ell_{1:G}$, is a vector of random probability measures $p_{1:G} = (p_1, \dots, p_G)$ where each p_g , with $g = 1, \dots, G$, is defined as in (2). We introduce the notation $p_{1:G} \sim \text{thinned-DDP}(\alpha, P_0, \ell_{1:G})$.

Definition 1 introduces a hierarchical construction for the vector $p_{1:G}$, where each component is a modified version of a shared DP p , introduced in (1), henceforth called the parent process p . This framework offers a hierarchical alternative to the well-known HDP (Teh et al. 2006), with a crucial difference: in the thinned-DDP, each marginal p_g is itself a DP with known parameters α and P_0 . In contrast, in the HDP, each element of the analog of $p_{1:G}$, while distributed as a DP conditionally on the realization of a common DP-distributed process, is characterized by a base measure that depends on that realization. The covariate-specific sequences $\ell_{1:G}$ act as a thinning mechanism that modifies the stick-breaking construction of parent process. Specifically, when $\ell_{j,g} = 0$, the corresponding weight $\omega_{j,g}$ is set to zero, and the atom θ_j is excluded from the construction of p_g . Using the stick-breaking metaphor from the definition of a DP, we can interpret $\omega_{j,g} = 0$ as indicating that, at the j th step, the stick used to define p_g is not broken. The resulting unassigned probability mass is redistributed by scaling all subsequent weights in p_g by a

factor of $(1 - v_j)^{-1}$, ensuring a well-defined random probability measure. The elements of $p_{1:G}$ are thus defined through the same set of atoms $(\theta_j)_{j \geq 1}$, but assign them different probabilities. This aligns with the single-atom DDP framework of [MacEachern \(2000\)](#), with the key distinction that, in the thinned-DDP construction, certain weights are exactly zero, a mechanism that explicitly models whether atoms are covariate-specific or shared. The thinned-DDP can thus be regarded as a limiting case of the single-atom DDP. In line with it, conditionally on the $\ell_{1:G}$, the random probability measures $p_{1:G}$ are identically distributed as a DP with concentration parameter α and base measure P_0 , the marginal distribution of each p_g being invariant to ℓ_g . The condition $\sum_{j=1}^{\infty} \ell_{j,g} = \infty$ indeed ensures that the unit stick is broken infinitely many times, with the weight generated the j th time the stick is actually broken having the same distribution as ω_j in (1). In addition, we observe that the thinned-DDP can also be framed as an instance of the general class of multivariate species sampling processes introduced by [Franzolini et al. \(2025\)](#).

We examine the mixed moments of a thinned-DDP, given the sequences $\ell_{1:G}$, to explore the dependence between pairs of elements in $p_{1:G}$. The next proposition characterizes the correlation between two random probability measures p_1 and p_2 jointly distributed as a thinned-DDP.

Proposition 1. *If $p_{1:2} \sim \text{thinned-DDP}(\alpha, P_0, \ell_{1:2})$, then, for any $A \in \mathcal{B}$, the correlation between $p_1(A)$ and $p_2(A)$ is given by*

$$\text{Corr}(p_1(A), p_2(A); \ell_{1:2}) = \frac{2}{(\alpha + 2)} \sum_{j \geq 1} \ell_{j,1} \ell_{j,2} \left(\frac{\alpha}{\alpha + 2} \right)^{s_j} \left(\frac{\alpha}{\alpha + 1} \right)^{q_j},$$

where $s_j = \sum_{h=1}^{j-1} \ell_{h,1} \ell_{h,2}$ and $q_j = \sum_{h=1}^{j-1} \mathbb{I}_{\{\ell_{h,1} \neq \ell_{h,2}\}}$ are, respectively, the number of shared and distribution-specific atoms in the first $j - 1$ components of $\ell_{1:2}$.

The correlation in Proposition 1 is expressed as an infinite sum, reflecting its dependence on the infinite sequences $\ell_{1:2}$. Within this sum, only the terms where both $\ell_{j,1}$ and $\ell_{j,2}$ are equal to one contribute to this quantity. Such correlation is always positive and spans the

entire interval $[0, 1]$, attaining a value of one when the sequences ℓ_1 and ℓ_2 are identical, and zero when there is no position in which both sequences simultaneously have a one. Additionally, the expression in Proposition 1 is independent of the choice of A , a measurable subset of Θ , which motivates the use of this correlation as a measure of dependence between the random probability measures p_1 and p_2 . This aligns with the findings of Franzolini et al. (2025), who showed that the same holds for the whole class of multivariate species sampling models. The result in Proposition 1 is readily adapted to study the correlation between a generic component of $p_{1:2}$ and the parent process p ; see Corollary D.1 in the Supplementary Material.

We conclude this section by analyzing the prior number of distinct values, or clusters, implied by a thinned-DDP model. The thinned-DDP allows for both common and covariate-specific atoms θ_j . Consequently, samples drawn from a thinned-DDP may share distinct values while also exhibiting values unique to specific components. To investigate this, we consider two samples, $y_{1,1}, \dots, y_{n_1,1} \mid p_{1:2} \stackrel{\text{iid}}{\sim} p_1$ and $y_{1,2}, \dots, y_{n_2,2} \mid p_{1:2} \stackrel{\text{iid}}{\sim} p_2$, where $p_{1:2} \sim \text{thinned-DDP}(\alpha, G_0, \ell_{1:2})$ for some pair of sequences $\ell_{1:2}$. We define K_0 as the number of distinct values shared between the two samples and let K_1 and K_2 represent the number of distinct values unique to the first and second samples, respectively. The total number of distinct values across both samples is thus given by $K = K_0 + K_1 + K_2$. To emphasize the dependence of K on n_1 , n_2 , and $\ell_{1:2}$, we introduce the notation $K(n_1, n_2; \ell_{1:2})$, which we use when convenient. We next focus on the prior expected value of K : while its exact form depends on the sequences $\ell_{1:2}$, it is nonetheless possible to establish bounds for it. The next result formalizes the intuitive idea that the expected total number of distinct values in two samples from a thinned-DDP falls between two extremes: (i) the expected number of distinct values in a single DP-distributed sample whose size equals the combined sizes of the two samples, and (ii) the sum of the expected number of distinct values in two independent DP-distributed samples.

Proposition 2. Let $y_{1,1}, \dots, y_{n_1,1} \mid p_{1:2} \stackrel{\text{iid}}{\sim} p_1$ and $y_{1,2}, \dots, y_{n_2,2} \mid p_{1:2} \stackrel{\text{iid}}{\sim} p_2$, where $p_{1:2} \sim \text{thinned-DDP}(\alpha, G_0, \ell_{1:2})$. Then

$$\sum_{i=1}^{n_1+n_2} \frac{i}{c+i-1} \leq \mathbb{E}[K(n_1, n_2; \ell_{1:2})] \leq \sum_{i=1}^{n_1} \frac{i}{c+i-1} + \sum_{i=1}^{n_2} \frac{i}{c+i-1}.$$

By combining Proposition 2 with the asymptotic analysis of the number of distinct values in samples from a DP (Korwar & Hollander 1973), we find that the growth of $\mathbb{E}[K(n_1, n_2; \ell_{1:2})]$, as $n_1 = n_2 = n \rightarrow \infty$, is bounded below by $\log(n)$ and above by $2 \log(n)$, with the bounds being sharp.

2.1 Eventually single-atom thinned-DDP

The thinned-DDP class has been introduced in its full generality, defined conditionally on G infinite sequences of thinning variables. However, simpler specifications can be achieved by imposing constraints on the structure of these sequences. For example, one may consider thinning sequences that eventually become constantly equal to one. Within this framework, a particularly simple case arises when each sequence ℓ_g consists of $u_g - 1$ initial zeros followed by an infinite sequence of ones. As a result, each p_g is defined as

$$p_g(\cdot) = \sum_{j=u_g}^{\infty} \left[v_j \prod_{h=u_g}^{j-1} (1 - v_h) \right] \delta_{\theta_j}(\cdot),$$

where u_g is, for any $g = 1, \dots, G$, a positive integer. We refer to the resulting distribution of the vector $p_{1:G}$ as the eventually single-atom thinned-DDP, reflecting the observation that all atoms θ_j with $j \geq \max(u_1, \dots, u_G)$ are shared among all components of $p_{1:G}$, and we introduce the notation $p_{1:G} \sim \text{thinned-DDP}(\alpha, P_0, u_{1:G})$, where $u_{1:G} = (u_1, \dots, u_G)$. This formulation implies a nested structure among the distributions. For example, if $G = 3$ and $u_1 < u_2 < u_3$, then p_3 includes only common atoms, p_2 includes an additional $u_3 - u_2$ atoms, shared with p_1 but not in p_3 , and p_1 includes a further $u_2 - u_1$ atoms unique to itself. The intuition behind this definition is that differences among distributions can be flexibly captured by the initial atoms in $\{\theta_j\}_{j \geq 1}$, which are those assigned the highest expected

probabilities. The simplicity of the eventually single-atom thinned-DDP is evident in the remarkably simple form that the correlation in Proposition 1 takes in this case. This is illustrated in the following result.

Corollary 1. *If $p_{1:2} \sim \text{thinned-DDP}(\alpha, P_0, u_{1:2})$, then, for any $A \in \mathcal{B}$, the correlation between $p_1(A)$ and $p_2(A)$ is given by*

$$\text{Corr}(p_1(A), p_2(A); u_{1:2}) = \left(\frac{\alpha}{\alpha + 1} \right)^{|u_2 - u_1|}.$$

The correlation depends on the sequences of thinning variables solely through the absolute difference between u_1 and u_2 , which represents the number of atoms not shared by p_1 and p_2 . Moreover, when $u_1 = u_2$, the correlation equals one, as $p_1 = p_2$. Conversely, as $|u_2 - u_1| \rightarrow \infty$, the correlation approaches zero, since the shared atoms contribute negligible probability in defining one of the distributions. Under the same assumptions, we can study the correlation between a component of $p_{1:2}$ and the parent process p ; see Corollary D.2 in the Supplementary Material.

Finally, the eventually single-atom thinned-DDP structure also allows us to derive an explicit expression for the prior expectation of the number of distinct values K , already studied in Propositions 2 for a generic thinned-DDP. This is formalized in the next proposition: although the expression may seem complex, its numerical evaluation is straightforward.

Proposition 3. *Let $y_{1,1}, \dots, y_{n_1,1} \mid p_{1:2} \stackrel{\text{iid}}{\sim} p_1$ and $y_{1,2}, \dots, y_{n_2,2} \mid p_{1:2} \stackrel{\text{iid}}{\sim} p_2$, where $p_{1:2} \sim \text{thinned-DDP}(\alpha, G_0, u_{1:2})$. If we assume that $u_1 \leq u_2$, then*

$$\begin{aligned} \mathbb{E}[K(n_1, n_2, u_{1:2})] &= \sum_{r=1}^{n_1} (-1)^{r-1} \binom{n_1}{r} \frac{\Gamma(\alpha + 1)\Gamma(r)}{\Gamma(\alpha + r)} \left(1 - \left(\frac{\alpha}{\alpha + r} \right)^{u_2 - u_1} \right) \\ &\quad + \sum_{r=0}^{n_1} \binom{n_1}{r} \left(\sum_{i=1}^{n_2 + n_1 - r} \frac{\alpha}{\alpha + i - 1} \right) \sum_{l=0}^r (-1)^l \binom{r}{l} \left(\frac{\alpha}{\alpha + l + n_1 - r} \right)^{u_2 - u_1}. \end{aligned}$$

We emphasize that although this section presents a specific example, the eventually single-atom thinned DDP can be extended to more general formulations that preserve tractability. One such formulation is described in Section C.2 of the Supplementary Material.

3 Priors for the thinning sequences

For practical application as a Bayesian model with G samples, it is convenient to combine the thinned-DDP with a prior distribution for the sequence $\ell_{1:G}$. Such prior should be specified to ensure the flexibility of the resulting Bayesian model. A particularly desirable property of a nonparametric model is its large support, which ensures that the model does not concentrate its probability mass on small subsets of probability measures. We next demonstrate that, under mild conditions on the prior distribution for $\ell_{1:G}$, the resulting thinned-DDP has full weak support. Conveniently, this implies that introducing dependence among the components of a vector of nonparametric priors via a thinned-DDP distribution preserves the flexibility of the DP in estimating the marginal distributions. Formally, we let $\mathcal{P}(\Theta)$ denote the set of all probability measures defined on (Θ, \mathcal{B}) , and $\mathcal{P}(\Theta)^G$ be the space of all G -dimensional vectors whose components take values in $\mathcal{P}(\Theta)$. We define $\mathcal{B}(\mathcal{P}(\Theta)^G)$ as the Borel σ -field generated by the product topology of weak convergence. The weak support of the thinned-DDP $p_{1:G}$ is then the smallest closed set in $\mathcal{B}(\mathcal{P}(\Theta)^G)$ to which $p_{1:G}$ assigns probability one. The next proposition establishes that, under mild conditions on the prior distribution on the thinning sequences, the weak support of the thinned-DDP coincides with $\mathcal{P}(\Theta)^G$. This result extends the comprehensive study of the support of the DDP by [Barrientos et al. \(2012\)](#) to the thinned-DDP case, which, as mentioned, can be seen as a limiting case of the class of DDP. Although the result is presented for the case $G = 2$, the extension to larger values of G is straightforward.

Proposition 4. *Let $p_{1:2} \sim \text{thinned-DDP}(\alpha, P_0, \ell_{1:2})$ be such that P_0 has full support on Θ , and assume that the sequences $\ell_{1:2}$ are assigned a prior distribution, independent of the sequences $\{\theta_j\}_{j \geq 1}$ and $\{v_j\}_{j \geq 1}$, that, for every $k \in \mathbb{N}$, assigns positive probability to the set*

$$\Omega_k = \{\ell_{j,1} = 1, \ell_{j,2} = 0 \text{ for } j = 1, \dots, k \text{ and } \ell_{j,2} = 1 \text{ for } j = k + 1, \dots, 2k\}. \quad (3)$$

Then $\mathcal{P}(\Theta)^G$ is the weak support of the process, i.e. the thinned-DDP has full weak support.

Condition (3) is very general, allowing for various prior specifications that satisfy it. In Sections 3.1 and 3.2, we thoroughly discuss two specific prior distributions for $\ell_{1:G}$ that meet this condition and thus lead to Bayesian models with full weak support. Two additional prior distributions are introduced in Sections C.1 and C.2.1 of the Supplementary Material.

3.1 Bernoulli thinning

A straightforward specification for the prior distribution of $\ell_{1:G}$ assumes independent Bernoulli priors for the elements of each covariate-specific sequence. Specifically, we let $\ell_{j,g} \stackrel{\text{iid}}{\sim} \text{Bern}(\pi_g)$, with $\pi_g \in (0, 1)$, for $j \geq 1$ and $g = 1, \dots, G$. We next characterize the correlation between pairs of distributions, marginalizing the thinning sequences.

Proposition 5. *Let $p_{1:2} \sim \text{thinned-DDP}(\alpha, P_0, \ell_{1:2})$ and consider a measurable set $A \in \mathcal{B}$. Assume $\ell_{j,1} \stackrel{\text{iid}}{\sim} \text{Bern}(\pi_1)$ and $\ell_{j,2} \stackrel{\text{iid}}{\sim} \text{Bern}(\pi_2)$ independent of each other, for $j \geq 1$. The correlation between $p_1(A)$ and $p_2(A)$ is*

$$\text{Corr}(p_1(A), p_2(A)) = \frac{2 \pi_1 \pi_2 (\alpha + 1)}{\alpha (\pi_1 + \pi_2) + 2(\pi_1 + \pi_2 - \pi_1 \pi_2)}.$$

Moreover, in the case $\pi_1 = \pi_2 = \pi$, the correlation simplifies to

$$\text{Corr}(p_1(A), p_2(A)) = \frac{\pi(\alpha + 1)}{\alpha + 2 - \pi}.$$

We observe that when $\pi_1 = \pi_2 = \pi = 1$, the two distributions are equal, and the correlation is one. As $\pi_1 = \pi_2 = \pi$ gets smaller, the probability of discarding atoms increases, and so does the probability of creating non-shared components, leading to a weaker correlation. Corollary D.3 in the Supplementary Material reports the correlation between a component of $p_{1:2}$ and the parent process p , under the same prior specification for $\ell_{1:2}$.

We now present a numerical investigation to assess how assigning a Bernoulli prior to the thinning sequences in a thinned-DDP affects the prior distribution of the number of distinct values, both shared across components and component-specific. Our analysis focuses on

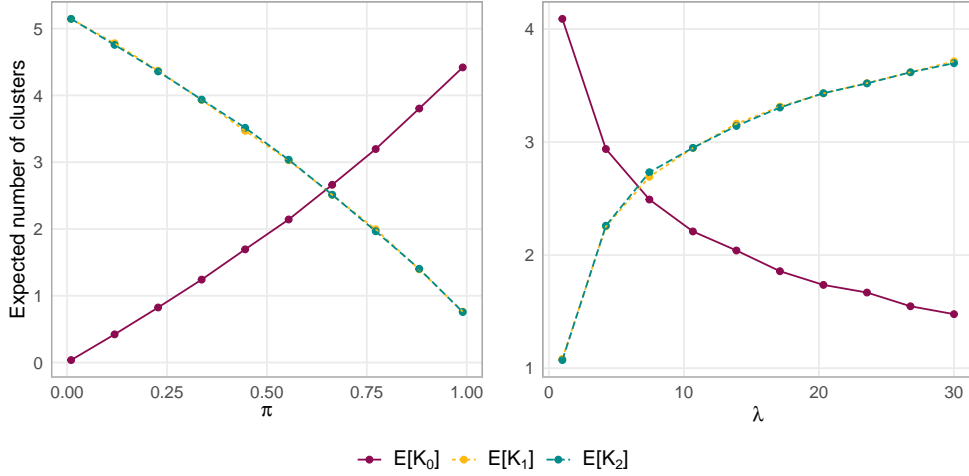


Figure 1: Expected number of shared clusters ($\mathbb{E}[K_0]$, continuous line) and covariate-specific clusters ($\mathbb{E}[K_1]$ and $\mathbb{E}[K_2]$, dashed lines) in two samples of size $n = 100$ from p_1 and p_2 , with $p_{1:2} \sim \text{thinned-DDP}(1, P_0, \ell_{1:2})$. Left: Bernoulli thinning, with π ranging in $(0, 1)$; Right: eventually single-atom Poisson thinning, with λ ranging in $(0, 30)$.

the case of $G = 2$ samples of size n from a vector $p_{1:2} \sim \text{thinned-DDP}(1, P_0, \ell_{1:2})$, with $\ell_{j,g} \stackrel{\text{iid}}{\sim} \text{Bern}(\pi)$ for $g = 1, 2$. The left panel of Figure 1 shows Monte Carlo estimates of $\mathbb{E}[K_0]$, $\mathbb{E}[K_1]$, and $\mathbb{E}[K_2]$ when $n = 100$ and for various values of the common thinning probability π in $(0, 1)$. When π is small, the expected number of shared clusters $\mathbb{E}[K_0]$ is close to zero. This occurs because both p_1 and p_2 are constructed by skipping most of the θ_j in (2), resulting in few atoms shared by p_1 and p_2 . As π increases, more atoms are common to p_1 and p_2 , leading to larger values of $\mathbb{E}[K_0]$. In contrast, the covariate-specific expected number of clusters, $\mathbb{E}[K_g]$ for $g = 1, 2$, exhibits the opposite behavior: since each p_g is marginally distributed as a DP with concentration parameter $\alpha = 1$, the estimated total expected number of distinct clusters within each sample, i.e. $\mathbb{E}[K_0] + \mathbb{E}[K_g]$, is approximately equal to $\sum_{i=1}^{100} 1/i \approx 5.19$ for all $\pi \in (0, 1)$. The left panel of Figure 2 illustrates the growth of the total expected number of clusters, $\mathbb{E}[K] = \mathbb{E}[K_0] + \mathbb{E}[K_1] + \mathbb{E}[K_2]$, as the sample size n increases. Interestingly, as π approaches the extremes of the interval $(0, 1)$, $\mathbb{E}[K]$ gets close to the bounds established in Proposition 2.

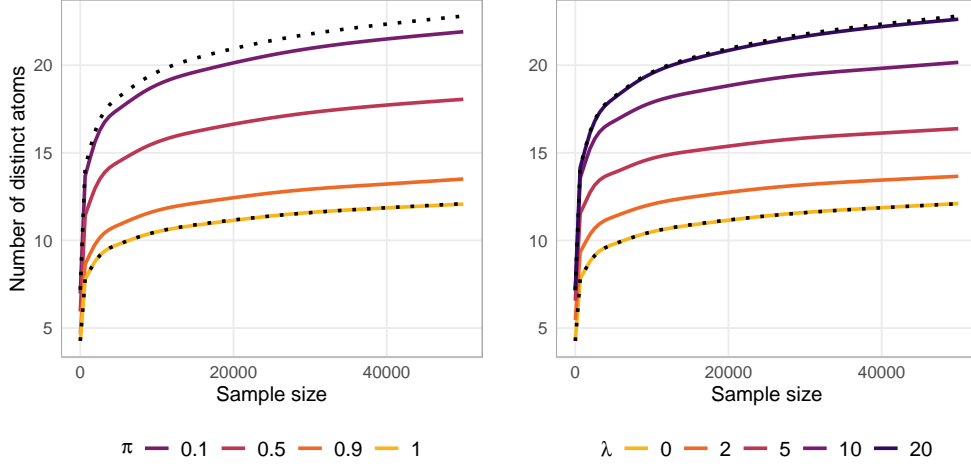


Figure 2: Total expected number of clusters, $\mathbb{E}[K]$, in two samples from p_1 and p_2 , with $p_{1:2} \sim \text{thinned-DDP}(1, P_0, \ell_{1:2})$, as a function of the size n of the two samples. Left: Bernoulli thinning, with π ranging in $\{0.1, 0.5, 0.9, 1\}$; Right: eventually single-atom Poisson thinning, with λ ranging in $\{0, 2, 5, 10, 20\}$. The dotted lines correspond to the theoretical bounds provided by Proposition 2.

3.2 Eventually single-atom Poisson thinning

In the eventually single-atom thinned-DDP, a prior for the number of atoms discarded by p_g , i.e., u_g , with $g = 1, 2$, is given by setting $u_g - 1 \stackrel{\text{ind}}{\sim} \text{Poisson}(\lambda_g)$. As in the previous section, we analyze the correlation between pairs of random probability measures $p_{1:2}$ by marginalizing with respect to u_1 and u_2 .

Proposition 6. *Let $p_{1:2} \sim \text{thinned-DDP}(\alpha, P_0, u_{1:2})$ and consider a measurable set $A \in \mathcal{B}$. Assume $u_g - 1 \stackrel{\text{ind}}{\sim} \text{Poisson}(\lambda_g)$, for $g = 1, 2$. The correlation between $p_1(A)$ and $p_2(A)$ is*

$$\text{Corr}(p_1(A), p_2(A)) = e^{-\lambda_1 - \lambda_2} \sum_{k=0}^{\infty} \left(\frac{\alpha}{1 + \alpha} \right)^k \left[\left(\frac{\lambda_1}{\lambda_2} \right)^{k/2} + \left(\frac{\lambda_2}{\lambda_1} \right)^{k/2} - \mathbb{I}_{\{0\}}(k) \right] I_k(2\sqrt{\lambda_1 \lambda_2}),$$

where I_k is the modified Bessel function of the first kind.

A simplification of the result presented in Proposition 6 arises by directly assigning a Poisson prior to the absolute difference of $u_2 - u_1$, e.g., $|u_2 - u_1| \sim \text{Poisson}(\lambda)$. In this case,

the correlation simplifies to

$$\text{Corr}(p_1(A), p_2(A)) = e^{-\lambda/(\alpha+1)}.$$

As apparent, the correlation approaches one as $\lambda \rightarrow 0$ and zero as $\lambda \rightarrow +\infty$. Under the same prior specification for $\ell_{1:2}$, Corollary D.4 in the Supplementary Material presents the correlation between a component of $p_{1:2}$ and the parent process p .

As in the previous section, we conduct a numerical analysis to examine how assigning a Poisson prior to the variables u_g in an eventually single-atom thinned-DDP influences the prior distribution of the number of distinct values, both shared across components and component-specific. Our analysis considers the same setting as in Section 3.1, except that here we assume $p_{1:2} \sim \text{thinned-DDP}(1, P_0, u_{1:2})$, with $u_g - 1 \stackrel{\text{iid}}{\sim} \text{Poisson}(\lambda)$ for $g = 1, 2$. The right panel of Figure 1 displays Monte Carlo estimates of $\mathbb{E}[K_0]$, $\mathbb{E}[K_1]$, and $\mathbb{E}[K_2]$ for $n = 100$ and various values of λ . When λ is small, the expected number of covariate-specific clusters, $\mathbb{E}[K_g]$, is close to zero. This occurs because the number of atoms not shared between p_1 and p_2 coincides with $|u_2 - u_1|$, and since both the distributions of u_1 and u_2 are concentrated around values close to zero, $|u_2 - u_1|$ has a small mean and variance. As λ increases, both the mean and variance of $|u_2 - u_1|$ grow, leading to a larger expected number of unshared atoms and, consequently, an increase in each $\mathbb{E}[K_g]$. Conversely, $\mathbb{E}[K_0]$ follows an opposite trend since the total expected number of clusters, $\mathbb{E}[K_0] + \mathbb{E}[K_g]$, is constant with respect to λ . The right panel of Figure 2 shows the growth of the total expected number of clusters, $\mathbb{E}[K]$, as the sample size n increases. This growth appears more rapid for larger values of λ . Additionally, as λ approaches zero or becomes large, $\mathbb{E}[K]$ gets close to the bounds established in Proposition 2.

4 Thinned-DDP mixture models

In view of the applications in Sections 5 and 6, we consider G samples of continuous observations, $y_g = (y_{1,g}, \dots, y_{n_g,g})$ for $g = 1, \dots, G$, and summarize the data in the n -dimensional vector $y_{1:G} = (y_1, \dots, y_G)$, where $n = n_1 + \dots + n_G$. When modeling continuous observations, the almost sure discreteness of the DP makes it unsuitable. A common approach is to convolve it with a continuous kernel. We propose modeling $y_{1:G}$ as partially exchangeable using a Gaussian mixture model with a thinned-DDP vector of mixing measures and Bernoulli priors for the thinning sequences. Namely,

$$\begin{aligned}
 y_g \mid f_g &\stackrel{\text{ind}}{\sim} f_g & g = 1, \dots, G \\
 f_g &= \phi * p_g & g = 1, \dots, G \\
 p_{1:G} &\sim \text{thinned-DDP}(\alpha, P_0, \ell_{1:G}) \\
 \ell_{j,g} &\stackrel{\text{iid}}{\sim} \text{Bern}(\pi_g) & j = 1, 2, \dots; g = 1, \dots, G
 \end{aligned} \tag{4}$$

where $\phi(\cdot) = \phi(\cdot \mid \mu, \sigma^2)$ is the density function of a Gaussian random variable with mean μ and variance σ^2 , and $*$ denotes the convolution operator. To ensure conjugacy, we specify the base measure P_0 as a normal-inverse gamma distribution with parameters $(\mu_0, \tau_0, \gamma_0, \lambda_0)$. Namely, $(\mu, \sigma^2) \sim P_0$ means that $\mu \mid \sigma^2 \sim \text{N}(\mu_0, \sigma^2/\tau_0)$ and $1/\sigma^2 \sim \text{Gamma}(\gamma_0, \lambda_0)$. The covariate-specific thinning probabilities π_g are assigned independent $\text{Beta}(a_\pi, b_\pi)$ priors.

Although our proposed framework is general, in model (4) and throughout the remainder of the paper, we focus on the Bernoulli thinning specification introduced in Section 3.1, as it yields the most straightforward computational scheme. Given the constructive definition in (2), we find it convenient to adapt computational strategies, originally devised for the DP, relying on its stick-breaking representation, to the partially exchangeable setting considered here. Notable examples from the literature include the blocked Gibbs sampler (Ishwaran & James 2001), the slice sampler and its efficient variants (Walker 2007, Kalli et al. 2011, Ge et al. 2015), and the retrospective sampler (Papaspiliopoulos & Roberts 2008). These methods, commonly referred to as conditional samplers, operate by explicitly updating

the process components within the sampler and rely on either stochastic or deterministic truncation. We outline a blocked Gibbs sampler for the thinned-DDP mixture model with Bernoulli thinning in (4). The conjugate specification of kernel ϕ and base measure P_0 allows for the analytical derivation of full conditional distributions for all model parameters. The main steps of our algorithm mirror those of a standard blocked Gibbs sampler for a Dirichlet process, with two key distinctions: (i) our approach explicitly updates the thinning sequences $\ell_{1:G}$, and (ii) the update of the common stick-breaking variables v_j accounts for observations across all samples y_g , with $g = 1, \dots, G$. The complete algorithm is detailed in Section E of the Supplementary Material.

5 Simulation studies

We conduct a numerical investigation of the posterior properties of the thinned-DDP mixture model defined in Section 4 using simulated data consisting of G samples. Specifically, we assess the accuracy of the estimated partitions of the observations and that of the posterior density estimates. The study is divided into two parts, presented in Sections 5.1 and 5.2. First, to illustrate how the thinned-DDP framework enables information sharing across groups while accounting for heterogeneity, we compare its results to two extreme modeling approaches: complete pooling and no pooling. In the complete-pooling approach, the data structure is ignored by combining all G samples into a single one and fitting a common DP mixture, thereby maximizing information sharing. This formulation corresponds to setting $\pi_g = 1$ for all groups in the thinned-DDP. On the other hand, the no-pooling approach adopts independent DP mixture models for the G samples, thus preventing any information sharing across them. Second, to assess the performance of the thinned-DDP, we compare its results with two state-of-the-art modeling approaches: the CAM of Denti et al. (2023) and the GM-DDP of Lijoi et al. (2014). Like the thinned-DDP, both the CAM and the GM-DDP can be used as nonparametric models for grouped data while also inducing a

partition of the entire data vector. Additionally, efficient algorithms for posterior inference are available for CAM and GM-DDP, implemented in the R packages `SANple` (D’Angelo & Denti 2023) and `BNPmix` (Corradin et al. 2021), respectively. These features ensure a fair and meaningful comparison with our proposed approach.

We simulated grouped data $y_{1:G}$, where each sample y_g , with $g = 1, \dots, G$, follows a finite mixture of univariate Gaussians. Specifically, each y_g was drawn from either a three-component mixture with means at $(-5, 0, 5)$ and probabilities $(0.5, 0.25, 0.25)$ or a two-component mixture with means at $(5, 10)$ and probabilities $(0.4, 0.6)$. The component variances were fixed at 0.6 across all mixtures. To evaluate how the number of groups and their sample sizes influence posterior inference, we considered multiple configurations. First, we generated data from $G = 2$ populations with varying sample sizes: $(n_1, n_2) = \{(10, 30), (20, 60), (30, 90), (40, 120)\}$. Next, we extended the analysis to $G = 10$ populations with sample sizes $(n_{g'}, n_{g''}) = \{(10, 30), (20, 60), (30, 90), (40, 120)\}$ with $g' = 1, \dots, 5$ and $g'' = 6, \dots, 10$. This setup resulted in total sample sizes n ranging from 40 to 800. In both scenarios, $G = 2$ and $G = 10$, half of the samples were drawn from the three-component mixture and the other half from the two-component mixture. Each experiment was repeated on 50 independent datasets. The algorithm settings and prior specifications are described in detail in Section F of the Supplementary Material.

5.1 Comparison with complete-pooling and no-pooling mixtures

We begin by evaluating the models’ ability to estimate the data partition. To do so, we use the realizations from the posterior distribution of the cluster allocation variables to construct group-specific posterior similarity matrices, where each entry (i, i') represents the posterior probability that observations i and i' , with $i, i' \in \{1, \dots, n_g\}$, belong to the same cluster within group g . Next, we obtain point estimates of the partitions by minimizing the variation of information loss (Wade & Ghahramani 2018), implemented

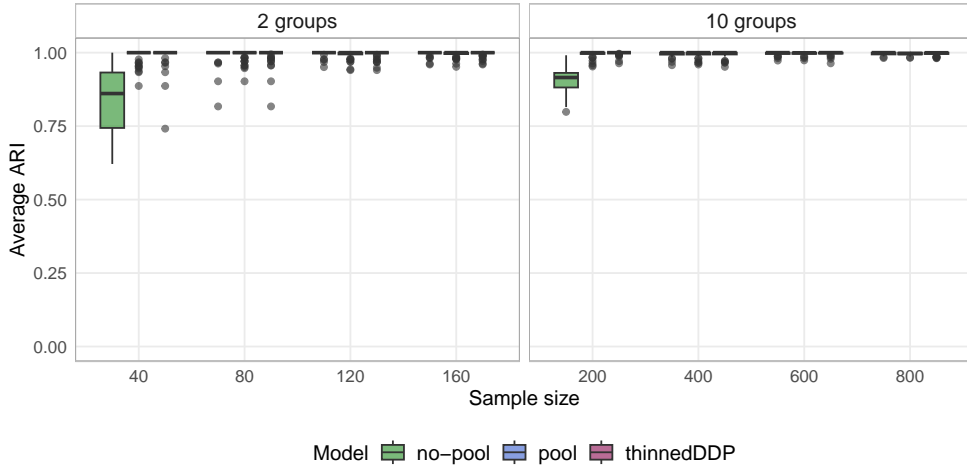


Figure 3: Boxplot of the average ARI for the thinned-DDP, the complete-pooling, and the no-pooling DP mixture on the simulated data.

via the `saIso` R package (Dahl et al. 2023, 2022). To assess accuracy, we compute the Adjusted Rand Index (ARI; Rand 1971, Hubert & Arabie 1985) for each group, measuring the agreement between the estimated and true partitions. As a summary measure, we report the average ARI, calculated as the mean of the group-specific ARIs. Figure 3 represents the distribution of the ARI across 50 replications for all combinations of G and n . The no-pooling model highlights a key limitation: when the sample size is small, the lack of information sharing between groups significantly impacts performance, leading to a lower ARI in the first configuration. In contrast, both the complete-pooling and thinned-DDP mixtures demonstrate strong performance in estimating the data partition in all settings.

Next, we evaluate the models' accuracy in estimating the data density. At each MCMC iteration $q = 1, \dots, Q$, we computed an estimate of f_g on a grid of 300 equally spaced points x_i , which we denote as $\hat{f}_g^{(q)}(x_i)$. The final density estimate at each x_i was then obtained as the Monte Carlo mean $\hat{f}_g(x_i) = \frac{1}{Q} \sum_{q=1}^Q \hat{f}_g^{(q)}(x_i)$. To assess the overall accuracy of the posterior point estimate, Figure 4 summarizes the distribution of the TV distance across scenarios. As expected, the complete pooling approach exhibits the largest discrepancy from the true density in all cases. When $G = 2$, the no-pooling and thinned-DDP models

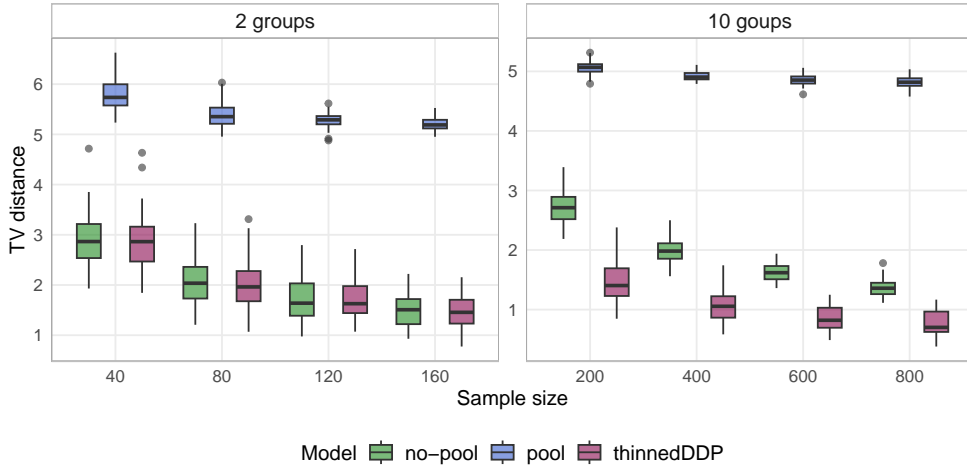


Figure 4: Boxplot of the TV distance for the thinned-DDP, the complete-pooling, and the no-pooling DP mixture on the simulated data.

demonstrate comparable accuracy. However, for $G = 10$, the thinned-DDP consistently achieves a smaller TV distance, particularly for small sample sizes. This improved accuracy in posterior density estimation is likely attributed to its ability to share information across groups. To assess the uncertainty of the estimates \hat{f}_g alongside their accuracy, we estimated pointwise 95% highest posterior density (HPD) credible intervals on the same grid. As an overall measure of uncertainty, we computed the average length of these intervals. Figure F2 in the Supplementary Material displays a summary of the distribution of this measure. The results clearly show that the thinned-DDP balances between the two extremes of complete and no pooling. The no-pooling model, relying solely on individual samples, exhibits the highest uncertainty, whereas the complete-pooling model, using all data, has the lowest. The thinned-DDP consistently falls between these extremes, demonstrating its ability to borrow information and reduce the variability of group-specific estimates.

5.2 Comparison with state-of-the-art methods

We now compare the thinned-DDP with two nonparametric mixture models for dependent grouped data: the CAM and the GM-DDP. As before, we begin by evaluating the models'

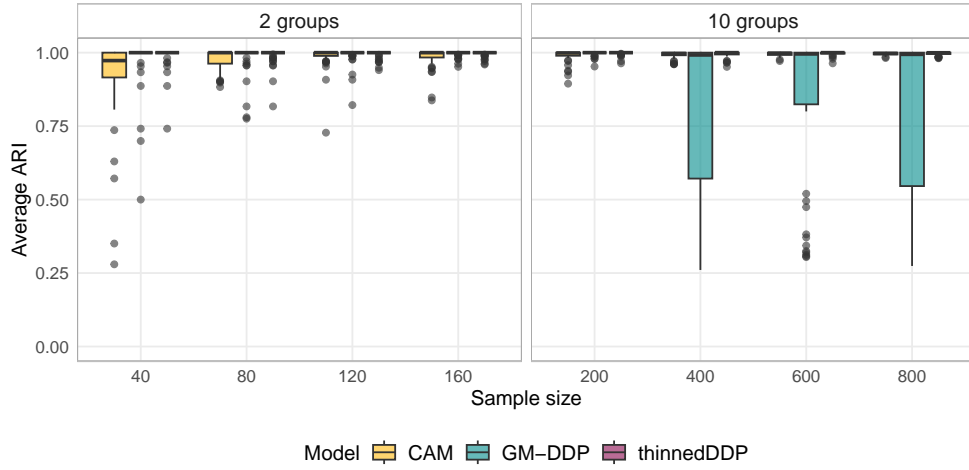


Figure 5: Boxplot of the average ARI for the thinned-DDP, the CAM, and the GM-DDP mixture on the simulated data.

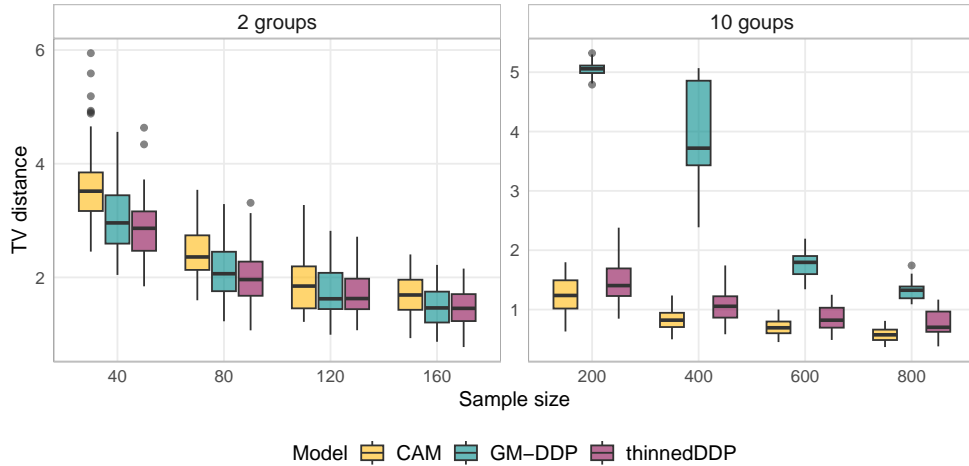


Figure 6: Boxplot of the TV distance for the thinned-DDP, the CAM, and the GM-DDP mixture on the simulated data.

ability to recover the true data partition. Figure 5 displays a summary of the distribution of the average ARI, as defined in the previous section, across all replications for each combination of G and sample sizes n_g , $g = 1, \dots, G$. Both the CAM and the thinned-DDP demonstrate strong performance across all scenarios, achieving near-perfect ARI in several configurations. While the GM-DDP performs comparably well when $G = 2$, it appears to struggle in settings with a larger number of populations and greater sample sizes.

Turning to the models’ ability to estimate the data density, Figure 6 provides a summary of the distribution of the TV distance, assessing the accuracy of the posterior point estimates, while Figure F3 in the Supplementary Material summarizes the distribution of the average size of the credible bands, evaluating the uncertainty associated with the estimates. When $G = 2$, all models exhibit similar performance; however, the thinned-DDP provides slightly more accurate and precise density estimates than its competitors. For $G = 10$, the CAM’s accuracy and precision improve steadily as the sample size increases, yet the thinned-DDP maintains comparable performance across all configurations. In contrast, when $G = 10$ and the sample size is small, the GM-DDP appears to struggle with density estimation. To further understand each model’s behavior and the rationale behind these results, it is useful to examine examples of the estimated densities and credible bands. Figures F4-F9 in the Supplementary Material illustrate these quantities for randomly selected datasets simulated under different settings. The graphs compare the posterior point estimates and credible bands of the densities obtained using the thinned-DDP, CAM, and GM-DDP, alongside the true data-generating density for reference. A visual inspection highlights that a key advantage of the thinned-DDP over CAM is its ability to prevent excessive information sharing between groups, particularly when populations are heterogeneous and samples are small. In such cases, CAM tends to introduce spurious modes. For $G = 2$, the GM-DDP also effectively avoids this issue. However, when the number of populations increases and sample sizes remain small, the additive structure of the GM-DDP limits its flexibility in capturing heterogeneity. To address this limitation, one could explore more refined formulations, such as those proposed in [Corradin et al. \(2019\)](#).

6 Real data analysis

The Collaborative Perinatal Project (CPP) was a large longitudinal study conducted in the United States between 1959 and 1965 to investigate the impact of pregnancy complications

on children’s health. It enrolled thousands of women from 12 medical centers across the country. Here, we focus on a subset of the data and analyze the gestational age of 2,313 women. While the distributions of this variable across the 12 centers share similar medians and right tails, their left tails differ noticeably. Some hospitals have a considerably higher proportion of patients with very short gestational ages (premature births) than others, suggesting that the hospital sample is not homogeneous. See Figure G10 in the Supplementary Material. Additionally, the sample sizes of the centers vary widely, ranging from 77 to 481 patients. Pooling data from multiple sources is essential in observational studies, offering significant advantages over single-center analyses, including larger sample sizes, greater population diversity, and improved generalizability. However, within each hospital, unobserved factors can influence patient outcomes, leading to potential heterogeneity among individuals in the same center. An effective model should account for these various sources of variability while flexibly integrating information across samples. The thinned-DDP mixture model is particularly well-suited for this task. Its mixture formulation captures latent heterogeneity within centers, while the presence of shared atoms effectively models similarities in the densities across samples. At the same time, both group-specific atoms and the group-specific weights of shared atoms account for differences, striking a balance between borrowing information and preserving individual center characteristics.

We estimated a thinned-DDP Gaussian mixture model with Bernoulli thinning, as described in Section 4, by running the blocked Gibbs Sampler for 10,000 iterations, discarding the first 5,000 as burn-in. The truncation parameter was set here equal to 300, while the remaining model parameters were set as in Section 5. The posterior point estimate of the partition provides a first valuable insight into the data. Thanks to the commonality of the atoms of the thinned-DDP, we can estimate the overall partition, alongside the group-specific ones, to allow for a better characterization of the patients across centers. Minimizing the variation of information loss results in three estimated clusters. The sam-

ple means of observations allocated to each cluster are equal to 33.9, 39.8, and 44.0 weeks. Hence, it is natural to interpret these clusters as the sub-populations of premature births, full-term standard pregnancies, and post-term pregnancies, respectively. In Figures 7, the bottom panels display the hospital-specific observations colored according to such partition, while the top panels show the histogram of the data, along with the densities' point estimates and 95% pointwise HPD credible intervals. The majority of observations in all hospitals are assigned to the cluster of standard pregnancies. On the contrary, the proportions of pre-term and post-term pregnancies vary significantly between centers. For instance, the distribution of Hospital 4 is predominantly explained by a single cluster, with a second component only used to account for two outliers. In contrast, Hospital 5 exhibits all three clusters, each with a significant number of observations. The density estimates highlight these differences in the weight of each sub-population across hospitals. Some densities appear symmetric and unimodal, while others display evident multimodality and skewness. This analysis demonstrates the flexibility of the thinned-DDP in capturing the heterogeneity both within the data, by identifying distinct sub-populations, and across groups, by accounting for discrepancies in the cluster weights between samples.

The estimated model and the algorithm's outputs further allow us to assess the similarity between hospital-specific densities. For each pair of hospitals, we can track whether they were modeled using the same mixture components over the iterations of the Gibbs sampler. Storing this information in a 12×12 matrix returns the frequencies with which each pair of hospitals was modeled by the same mixture density. This matrix can be interpreted as a posterior similarity matrix and used to perform clustering of the hospitals. Minimizing the variation of information loss, we identified two distinct clusters: the first includes Hospitals 2, 4, and 7, while the second comprises the remaining hospitals. Notably, hospitals in the first cluster are characterized by significantly fewer points assigned to the observational clusters for pre-term and post-term pregnancies. This finding aligns

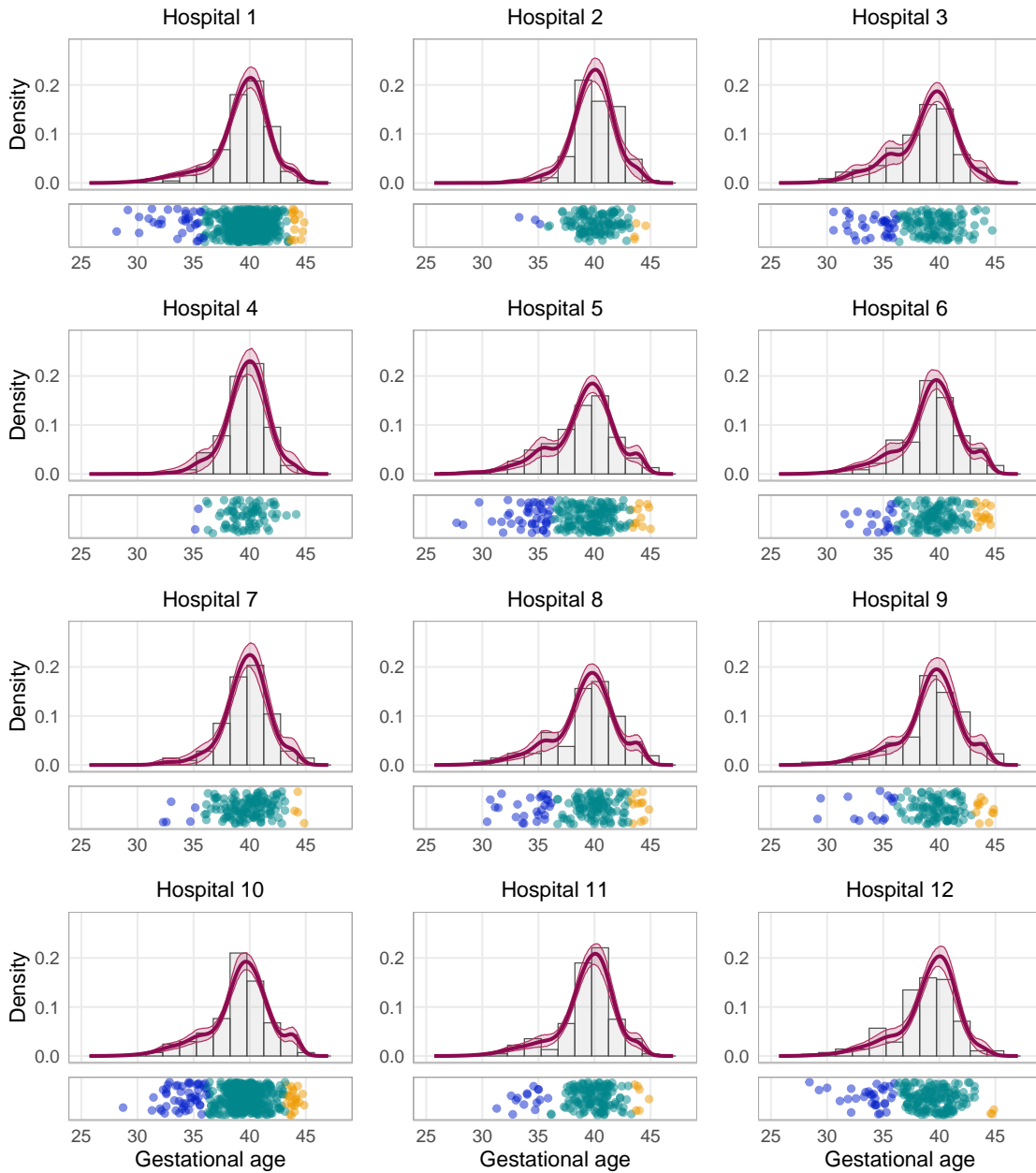


Figure 7: Top panels: histogram of the data, posterior density estimate via thinned-DDP (continuous line) and 95% pointwise HPD credible intervals (shaded area) for each hospital. Bottom panels: jittered observations, colored by estimated cluster allocation.

with the estimated total variation distance computed across the group-specific densities, as shown in Figure G11 in the Supplementary Material. The plot displays the Monte Carlo estimate of the TV distance between all pairs of hospitals and highlights two distinct blocks of hospitals with similar densities.

References

- Barrientos, A. F., Jara, A. & Quintana, F. A. (2012), ‘On the Support of MacEachern’s Dependent Dirichlet Processes and Extensions’, *Bayesian Analysis* **7**(2), 277 – 310.
- Bi, D. & Ji, Y. (2024), ‘A Class of Dependent Random Distributions Based on Atom Skipping’, *arXiv preprint arXiv:2304.14954* pp. 1 – 43.
- Camerlenghi, F., Dunson, D. B., Lijoi, A., Prünster, I. & Rodríguez, A. (2019), ‘Latent Nested Nonparametric Priors (with Discussion)’, *Bayesian Analysis* **14**(4), 1303.
- Corradin, R., Canale, A. & Nipoti, B. (2019), Galaxy Color Distribution Estimation via Dependent Nonparametric Mixtures, in ‘Book of Short Papers SIS 2019’, pp. 713 – 718.
- Corradin, R., Canale, A. & Nipoti, B. (2021), ‘BNPmix: An R Package for Bayesian non-parametric modeling via Pitman-Yor mixtures’, *Journal of Statistical Software* **100**(15), 1 – 33.
- Dahl, D. B., Johnson, D. J. & Müller, P. (2022), ‘Search Algorithms and Loss Functions for Bayesian Clustering’, *Journal of Computational and Graphical Statistics* **31**, 1189 – 1201.
- Dahl, D. B., Johnson, D. J. & Müller, P. (2023), *salso: Search Algorithms and Loss Functions for Bayesian Clustering*. R package, version 0.3.35.
URL: <https://CRAN.R-project.org/package=salso>
- D’Angelo, L. & Denti, F. (2023), *SANple: Fitting Shared Atoms Nested Models via Markov Chains Monte Carlo*. R package, version 0.1.0.
URL: <https://CRAN.R-project.org/package=SANple>
- Denti, F., Camerlenghi, F., Guindani, M. & Mira, A. (2023), ‘A Common Atoms Model

- for the Bayesian Nonparametric Analysis of Nested Data’, *Journal of the American Statistical Association* **118**(541), 405 – 416.
- Duan, J. A., Guindani, M. & Gelfand, A. E. (2007), ‘Generalized Spatial Dirichlet Process Models’, *Biometrika* **94**(4), 809 – 825.
- Franzolini, B., Lijoi, A., Prünster, I. & Rebaudo, G. (2025), ‘Multivariate Species Sampling Models’, *arXiv preprint arXiv:2503.24004* pp. 1 – 24.
- Fuentes, M. & Reich, B. (2013), ‘Multivariate Spatial Nonparametric Modelling via Kernel Processes Mixing’, *Statistica Sinica* **23**(1), 75 – 97.
- Ge, H., Chen, Y., Wan, M. & Ghahramani, Z. (2015), Distributed Inference for Dirichlet Process Mixture Models, *in* ‘International Conference on Machine Learning’, PMLR, pp. 2276–2284.
- Griffin, J. E. & Steel, M. F. J. (2006), ‘Order-Based Dependent Dirichlet Processes’, *Journal of the American Statistical Association* **101**(473), 179 – 194.
- Griffin, J. E. & Steel, M. F. J. (2011), ‘Stick-Breaking Autoregressive Processes’, *Journal of Econometrics* **162**(2), 383 – 396.
- Hubert, L. & Arabie, P. (1985), ‘Comparing Partitions’, *Journal of Classification* **2**, 193 – 218.
- Ishwaran, H. & James, L. F. (2001), ‘Gibbs Sampling Methods for Stick-Breaking Priors’, *Journal of the American statistical Association* **96**(453), 161–173.
- Kalli, M., Griffin, J. E. & Walker, S. G. (2011), ‘Slice Sampling Mixture Models’, *Statistics and Computing* **21**, 93 – 105.
- Korwar, R. M. & Hollander, M. (1973), ‘Contributions to the Theory of Dirichlet Processes’, *The Annals of Probability* **1**(4), 705–711.

- Lau, J. W. & Cripps, E. (2022), ‘Thinned Completely Random Measures with Applications in Competing Risks Models’, *Bernoulli* **28**(1), 638 – 662.
- Lijoi, A., Nipoti, B. & Prünster, I. (2014), ‘Bayesian Inference with Dependent Normalized Completely Random Measures’, *Bernoulli* **20**(3), 1260 – 1291.
- MacEachern, S. N. (2000), ‘Dependent Dirichlet processes’, *Unpublished manuscript, Department of Statistics, The Ohio State University* **5**.
- Papaspiliopoulos, O. & Roberts, G. O. (2008), ‘Retrospective Markov Chain Monte Carlo Methods for Dirichlet Process Hierarchical Models’, *Biometrika* pp. 169–186.
- Pitman, J. (2006), *Combinatorial Stochastic Processes: Ecole d’été de Probabilités de Saint-Flour xxxii-2002*, Springer Science & Business Media.
- Quintana, F. A., Müller, P., Jara, A. & MacEachern, S. N. (2022), ‘The Dependent Dirichlet Process and Related Models’, *Statistical Science* **37**(1), 24 – 41.
- Rand, W. M. (1971), ‘Objective Criteria for the Evaluation of Clustering Methods’, *Journal of the American Statistical Association* **66**(336), 846 – 850.
- Sethuraman, J. (1994), ‘A Constructive Definition of Dirichlet Priors’, *Statistica Sinica* **4**(2), 639 – 650.
- Teh, Y. W., Jordan, M. I., Beal, M. J. & Blei, D. M. (2006), ‘Hierarchical Dirichlet Processes’, *Journal of the American Statistical Association* **101**(476), 1566 – 1581.
- Wade, S. & Ghahramani, Z. (2018), ‘Bayesian Cluster Analysis: Point Estimation and Credible Balls (with Discussion)’, *Bayesian Analysis* **13**(2), 559 – 626.
- Walker, S. G. (2007), ‘Sampling the Dirichlet Mixture Model with Slices’, *Communications in Statistics - Simulation and Computation* **36**(1), 45 – 54.

Zeng, C., Miller, J. W. & Duan, L. L. (2023), ‘Consistent Model-Based Clustering Using the Quasi-Bernoulli Stick-Breaking Process’, *Journal of Machine Learning Research* **24**(153), 1 – 32.

Supplementary Material

A Proofs of the results in Section 2

A.1 Proof of Proposition 1

We derive the correlation between pairs of distributions distributed as a thinned-DDP. Since the thinned-DDP belongs to the class of multivariate species sampling processes introduced by [Franzolini et al. \(2025\)](#), we can specialize their Proposition 2.7 to our setting. Specifically, Proposition 2.7 states that, if (p_1, p_2) are distributed as a multivariate species sampling process, then, for every measurable set A such that $0 < P_0(A) < 1$,

$$\text{Corr}(p_1(A), p_2(A)) = \frac{\Pr(y_{i,1} = y_{k,2})}{\sqrt{\Pr(y_{i,1} = y'_{i',1})\Pr(y_{k,2} = y'_{k',2})}}. \quad (5)$$

Consider $p_{1:2} \sim \text{thinned-DDP}(\alpha, P_0, \ell_{1:2})$, then $\Pr(y_{i,g} = \theta_j \mid p_g) = v_j \ell_{j,g} \prod_{m < j} (1 - v_m \ell_{m,g})$, for $j \geq 1$ and $g = 1, 2$. We start by computing the numerator of Eq. (5).

$$\begin{aligned} \Pr(y_{i,1} = y_{k,2} \mid p_1, p_2) &= \sum_{j \geq 1} \Pr(y_{i,1} = j, y_{k,2} = j \mid p_1, p_2) \\ &= \sum_{j \geq 1} \Pr(y_{i,1} = j \mid p_1, p_2) \Pr(y_{k,2} = j \mid p_1, p_2) \\ &= \sum_{j \geq 1} [\ell_{j,1} v_j \prod_{h < j} (1 - \ell_{h,1} v_h)] [\ell_{j,2} v_j \prod_{h < j} (1 - \ell_{h,2} v_h)] \\ &= \sum_{j \geq 1} \ell_{j,1} \ell_{j,2} v_j^2 \prod_{h < j} (1 - \ell_{h,1} v_h) (1 - \ell_{h,2} v_h) \\ &= \sum_{j \geq 1} \ell_{j,1} \ell_{j,2} v_j^2 \prod_{h < j} \left(1 - (\ell_{h,1} + \ell_{h,2}) v_h + \ell_{h,1} \ell_{h,2} v_h^2 \right). \end{aligned}$$

Marginalizing with respect to $\{v_j\}_{j \geq 1}$ we get

$$\begin{aligned} \Pr(y_{i,1} = y_{k,2}; \ell_{1:2}) &= \sum_{j \geq 1} \ell_{j,1} \ell_{j,2} \mathbb{E}[v_j^2] \prod_{h < j} \left(1 - (\ell_{h,1} + \ell_{h,2}) \mathbb{E}[v_h] + \ell_{h,1} \ell_{h,2} \mathbb{E}[v_h^2] \right) \\ &= \sum_{j \geq 1} \ell_{j,1} \ell_{j,2} \frac{2}{(\alpha + 1)(\alpha + 2)} \prod_{h < j} \left(1 - (\ell_{h,1} + \ell_{h,2}) \frac{1}{\alpha + 1} + \ell_{h,1} \ell_{h,2} \frac{2}{(\alpha + 1)(\alpha + 2)} \right) \end{aligned}$$

$$= \frac{2}{(\alpha+1)(\alpha+2)} \sum_{j \geq 1} \ell_{j,1} \ell_{j,2} \prod_{h < j} \frac{1}{(\alpha+1)(\alpha+2)} \underbrace{\left(\alpha^2 + 3\alpha + 2 - (\alpha+2)(\ell_{h,1} + \ell_{h,2}) + 2\ell_{h,1}\ell_{h,2} \right)}_{(a_h)}.$$

The last term depends on the specific realization of $\ell_{1:2}$. In particular, the quantity within braces is equal to

$$(a_h) = \begin{cases} \alpha(\alpha+2) & \text{if } \ell_{h,1} \neq \ell_{h,2} \\ (\alpha+1)(\alpha+2) & \text{if } \ell_{h,1} = \ell_{h,2} = 0 \\ \alpha(\alpha+1) & \text{if } \ell_{h,1} = \ell_{h,2} = 1 \end{cases}$$

which implies that

$$\frac{(a_h)}{(\alpha+1)(\alpha+2)} = \frac{\alpha}{\alpha + \ell_{h,1} + \ell_{h,2}}.$$

So we can write

$$\Pr(y_{i,1} = y_{k,2}; \ell_{1:2}) = \frac{2}{(\alpha+1)(\alpha+2)} \sum_{j \geq 1} \ell_{j,1} \ell_{j,2} \prod_{h < j} \frac{\alpha}{\alpha + \ell_{h,1} + \ell_{h,2}}.$$

Finally, to compute the correlation we need the denominator of (5), which is the product of the probabilities of observing ties within the same group. Since each p_g is distributed as a Dirichlet process, we have $\Pr(y_{i,g} = y_{i',g}) = 1/(\alpha+1)$.

Hence the correlation is

$$\text{Corr}(p_1(A), p_2(A); \ell_{1:2}) = \frac{2}{(\alpha+2)} \sum_{j \geq 1} \ell_{j,1} \ell_{j,2} \prod_{h < j} \frac{\alpha}{\alpha + \ell_{h,1} + \ell_{h,2}}.$$

Denoting with $s_j = \sum_{h=1}^{j-1} \ell_{h,1} \ell_{h,2}$ and $q_j = \sum_{h=1}^{j-1} \mathbb{I}_{\{\ell_{h,1} \neq \ell_{h,2}\}}$, the correlation can be further simplified into

$$\text{Corr}(p_1(A), p_2(A); \ell_{1:2}) = \frac{2}{(\alpha+2)} \sum_{j \geq 1} \ell_{j,1} \ell_{j,2} \left(\frac{\alpha}{\alpha+2} \right)^{s_j} \left(\frac{\alpha}{\alpha+1} \right)^{q_j}.$$

A.2 Proof of Proposition 2

We let $y_g = \{y_{1,g}, \dots, y_{n_g,g}\}$, with $g = 1, 2$, and $y = \{y_{1,1}, \dots, y_{n_1,1}, y_{1,2}, \dots, y_{n_2,2}\}$. We recall that

- $K = K(n_1, n_2; \ell_{1:2})$ is the number of distinct values in y ;
- $K_0 = K_0(n_1, n_2; \ell_{1:2})$ is the number of distinct values in y coinciding with observations in both y_1 and y_2 ;
- $K_g = K_g(n_g; \ell_{1:2})$ is the number of distinct values in y_g that do not coincide with any observation in y_{3-g} .

Moreover, we introduce:

- $K_g^{(g)}(n_g; \ell_{1:2})$ is the number of distinct values in y_g corresponding to atoms θ_j that are specific to p_g , that is for which $\ell_{j,g} = 1$ and $\ell_{j,3-g} = 0$;
- $K_0^{(g)}(n_g; \ell_{1:2})$ is the number of distinct values in y_g corresponding to atoms θ_j appearing in both p_1 and p_2 , that is for which $\ell_{j,1} = \ell_{j,2} = 1$;
- $K_0^{(1:2)}(n_1, n_2; \ell_{1:2})$ is the number of distinct values in y corresponding to atoms θ_j appearing in both p_1 and p_2 , that is for which $\ell_{j,1} = \ell_{j,2} = 1$;
- $K^{(g)}(n_g; \ell_{1:2}) = K_0^{(g)}(n_g; \ell_{1:2}) + K_g^{(g)}(n_g; \ell_{1:2})$ is the number of distinct values in y_g .

We observe that

$$K(n_1, n_2; \ell_{1:2}) = K_0^{(1:2)}(n_1, n_2; \ell_{1:2}) + K_1^{(1)}(n_1; \ell_{1:2}) + K_2^{(2)}(n_2; \ell_{1:2}), \quad (6)$$

almost surely, and that

$$K_0^{(1:2)}(n_1, n_2; \ell_{1:2}) = K_0^{(1)}(n_1; \ell_{1:2}) + K_0^{(2)}(n_2; \ell_{1:2}) - K_0(n_1, n_2; \ell_{1:2}), \quad (7)$$

almost surely. Equation 7 implies that, almost surely,

$$K_0^{(1:2)}(n_1, n_2; \ell_{1:2}) \leq K_0^{(1)}(n_1; \ell_{1:2}) + K_0^{(2)}(n_2; \ell_{1:2}). \quad (8)$$

From (6) and (8) we get that, almost surely,

$$K(n_1, n_2; \ell_{1:2}) \leq \sum_{g=1}^2 \left(K_0^{(g)}(n_g; \ell_{1:2}) + K_g^{(g)}(n_g; \ell_{1:2}) \right)$$

$$= \sum_{g=1}^2 K^{(g)}(n_g; \ell_{1:2}).$$

Thus,

$$\mathbb{E}[K(n_1, n_2; \ell_{1:2})] \leq \sum_{g=1}^2 \mathbb{E}[K^{(g)}(n_g; \ell_{1:2})] = \sum_{i=1}^{n_1} \frac{\alpha}{\alpha + i - 1} + \sum_{i=1}^{n_2} \frac{\alpha}{\alpha + i - 1},$$

where the last identity holds as, regardless of $\ell_{1:2}$, each p_g is marginally distributed as a DP with concentration parameter α for which we have $\mathbb{E}[K^{(g)}(n_g; \ell_{1:2})] = \sum_{i=1}^{n_g} \alpha / (\alpha + i - 1)$ (see [Pitman 2006](#)).

Next, we observe that the distribution of $K^{(g)}(n_g; \ell_{1:2})$ is invariant to the specification of $\ell_{1:2}$, as p_g is marginally distributed as a DP with concentration parameter α for any specification of $\ell_{1:2}$. As a consequence, we can write

$$\mathbb{E}[K^{(g)}(n_g; \ell_{1:2})] = \mathbb{E}[K^{(g)}(n_g; \tilde{\ell}_{1:2})] \tag{9}$$

where $\tilde{\ell}_{1:2}$ is such that the two sequences $\tilde{\ell}_1$ and $\tilde{\ell}_2$ are identical. The same definition of $\tilde{\ell}_{1:2}$ gives rise to the following two almost sure identities:

$$K_g^{(g)}(n_g; \tilde{\ell}_{1:2}) = 0, \tag{10}$$

$$K_0^{(1:2)}(n_1, n_2; \tilde{\ell}_{1:2}) = K(n_1, n_2; \tilde{\ell}_{1:2}). \tag{11}$$

By combining (6) and (7) we get

$$\begin{aligned} K(n_1, n_2; \ell_{1:2}) &= \sum_{g=1}^2 K_0^{(g)}(n_g; \ell_{1:2}) - K_0(n_1, n_2; \ell_{1:2}) + \sum_{g=1}^2 K_g^{(g)}(n_g; \ell_{1:2}) \\ &= \sum_{g=1}^2 K^{(g)}(n_g; \ell_{1:2}) - K_0(n_1, n_2; \ell_{1:2}). \end{aligned}$$

By taking the expectation of both sides of the last identity, we get

$$\begin{aligned} \mathbb{E}[K(n_1, n_2; \ell_{1:2})] &= \sum_{g=1}^2 \mathbb{E}[K^{(g)}(n_g; \ell_{1:2})] - \mathbb{E}[K_0(n_1, n_2; \ell_{1:2})] \\ &\stackrel{(9)}{=} \sum_{g=1}^2 \mathbb{E}[K^{(g)}(n_g; \tilde{\ell}_{1:2})] - \mathbb{E}[K_0(n_1, n_2; \ell_{1:2})] \end{aligned}$$

$$\begin{aligned}
&\geq \sum_{g=1}^2 \mathbb{E}[K^{(g)}(n_g; \tilde{\ell}_{1:2})] - \mathbb{E}[K_0(n_1, n_2; \tilde{\ell}_{1:2})] \\
&\stackrel{(10)}{=} \sum_{g=1}^2 \mathbb{E}[K_0^{(g)}(n_g; \tilde{\ell}_{1:2}) + K_g^{(g)}(n_g; \tilde{\ell}_{1:2})] - \mathbb{E}[K_0(n_1, n_2; \tilde{\ell}_{1:2})] \\
&= \mathbb{E} \left[\sum_{g=1}^2 K_0^{(g)}(n_g; \tilde{\ell}_{1:2}) \right] - \mathbb{E}[K_0(n_1, n_2; \tilde{\ell}_{1:2})] \\
&\stackrel{(7)}{=} \mathbb{E}[K_0^{(1:2)}(n_1, n_2; \tilde{\ell}_{1:2}) + K_0(n_1, n_2; \tilde{\ell}_{1:2})] - \mathbb{E}[K_0(n_1, n_2; \tilde{\ell}_{1:2})] \\
&\stackrel{(11)}{=} \mathbb{E}[K(n_1, n_2; \tilde{\ell}_{1:2})] \\
&\stackrel{(a)}{=} \sum_{i=1}^{n_1+n_2} \frac{\alpha}{\alpha + i - 1},
\end{aligned}$$

where (a) holds since the specification of $\tilde{\ell}_{1:g}$ implies a framework of complete pooling with a single sample y of size $n_1 + n_2$ distributed according to a DP with concentration parameter α .

A.3 Proof of Corollary 1

We derive the correlation between $p_1(A)$ and $p_2(A)$, where $p_{1:2} \sim \text{thinned-DDP}(\alpha, P_0, u_{1:2})$. We can specify the correlation in Proposition 1 for this setting by noting that, with this formulation, the first $\min\{u_1, u_2\}$ atoms are discarded from both distributions, the second $|u_2 - u_1|$ are distribution-specific, while the remaining ones are shared. Since the only components contributing to the correlation are the ones for which both $\ell_{j,1}$ and $\ell_{j,2}$ are non-zero, we are left with a sum for $j \geq \max\{u_1, u_2\}$. Moreover, at the generic index j in this set, $s_j = j - \max\{u_1, u_2\}$ and $q_j = |u_2 - u_1|$. Hence we obtain

$$\begin{aligned}
\text{Corr}(p_1(A), p_2(A); u_1, u_2) &= \frac{2}{\alpha + 2} \left(\frac{\alpha}{\alpha + 1} \right)^{|u_2 - u_1|} \sum_{j \geq \max\{u_1, u_2\}} \left(\frac{\alpha}{\alpha + 2} \right)^{j - \max\{u_1, u_2\}} \\
&= \frac{2}{\alpha + 2} \left(\frac{\alpha}{\alpha + 1} \right)^{|u_2 - u_1|} \frac{\alpha + 2}{2} \\
&= \left(\frac{\alpha}{\alpha + 1} \right)^{|u_2 - u_1|}.
\end{aligned}$$

A.4 Proof of Proposition 3

Without loss of generality, we assume $u_1 = 1$ and set $w = u_2 - u_1$. Thus we have that all the atoms in p_2 are shared by p_1 , while the first w atoms of p_1 , that is $\theta_{1:w} = \{\theta_1, \dots, \theta_w\}$, are not shared by p_2 . We introduce the random variable B consisting of the number of observations in $\{y_{1,1}, \dots, y_{n_1,1}\}$ that coincides with one element of $\theta_{1:w}$. Moreover, we let $K^{1:w}$ be number of distinct values among these B observations, and $K^{(w+1):\infty}$ the number of distinct values among the remaining $n_1 - B + n_2$ observations in $\{y_{1,1}, \dots, y_{n_1,1}, y_{1,2}, \dots, y_{n_2,2}\}$ that do not coincide with any of the atoms in $\theta_{1:w}$. We thus have

$$\mathbb{E}[K(n_1, n_2, u_{1:2})] = \mathbb{E}[K^{1:w}] + \mathbb{E}[K^{(w+1):\infty}]. \quad (12)$$

We let $v = (v_j)_{j \geq 1}$ and we start by working on the term $\mathbb{E}[K^{1:w}]$, for which we have

$$\begin{aligned} \mathbb{E}[K^{1:w}] &= \mathbb{E}_v[\mathbb{E}[K^{1:w} \mid v]] \\ &= \mathbb{E}_v \left[w - \sum_{j=1}^w (1 - \omega_j)^{n_1} \right] \\ &= w - \sum_{j=1}^w \mathbb{E}_v [(1 - \omega_j)^{n_1}] \\ &= w - \sum_{j=1}^w \mathbb{E}_v \left[\sum_{r=0}^{n_1} \binom{n_1}{r} (-1)^r \omega_j^r \right] \\ &= w - \sum_{j=1}^w \sum_{r=0}^{n_1} \binom{n_1}{r} (-1)^r \mathbb{E}_v [\omega_j^r] \\ &\stackrel{(a)}{=} w - \sum_{r=0}^{n_1} \binom{n_1}{r} (-1)^r \frac{\Gamma(1+r)\Gamma(\alpha)}{\Gamma(1+\alpha+r)} \sum_{j=1}^w \frac{\alpha^j}{(\alpha+r)^{j-1}} \\ &\stackrel{(b)}{=} w - \sum_{r=1}^{n_1} (-1)^r \binom{n_1}{r} \frac{\Gamma(1+r)\Gamma(\alpha)}{\Gamma(1+\alpha+r)} \frac{\alpha}{r} \frac{(\alpha+r)^w - \alpha^w}{(\alpha+r)^{w-1}} \\ &= w - \Gamma(\alpha+1) \sum_{r=1}^{n_1} (-1)^{r-1} \binom{n_1}{r} \frac{\Gamma(r)}{\Gamma(\alpha+r)} \left\{ 1 - \left(\frac{\alpha}{\alpha+r} \right)^w \right\}, \quad (13) \end{aligned}$$

where the (a) holds as

$$\mathbb{E}_v [\omega_j^r] = \mathbb{E}_v \left[v_j^r \prod_{l=1}^{j-1} (1 - v_l)^r \right],$$

with $v_j \stackrel{\text{iid}}{\sim} \text{Beta}(1, \alpha)$ for all $j = 1, 2, \dots$; and (b) holds as

$$\sum_{j=1}^w \frac{\alpha^{j-1}}{(\alpha+r)^{j-1}} = \begin{cases} w & \text{if } r = 0, \\ \frac{1}{r} \frac{(\alpha+r)^w - \alpha^w}{(\alpha+r)^{w-1}} & \text{if } r \geq 1. \end{cases}$$

Moreover, we observe that

$$\begin{aligned} \mathbb{E}[K^{(w+1):\infty}] &= \mathbb{E}_v [\mathbb{E}_{B|v} [\mathbb{E}[K^{(w+1):\infty} | B, v]]] \\ &= \mathbb{E}_v \left[\sum_{m=0}^{n_1} \mathbb{E}[K^{(w+1):\infty} | B = m, v] \Pr(B = m | v) \right] \\ &\stackrel{(c)}{=} \sum_{m=0}^{n_1} \mathbb{E}_v [\mathbb{E}[K^{(w+1):\infty} | B = m, v]] \mathbb{E}_v [\Pr(B = m | v)], \end{aligned} \quad (14)$$

where (c) holds as the distribution of B only depends on the the first w elements of the sequence v , say $v_{1:w}$, while, conditionally on $B = m$, the distribution of $K^{(w+1):\infty}$ only depends on the remaining elements of the sequence v , say $v_{(w+1):\infty}$. Moreover, we have

$$\begin{aligned} \mathbb{E}_v [\Pr(B = m | v)] &= \mathbb{E}_{v_{1:w}} [\Pr(B = m | v_{1:w})] \\ &= \mathbb{E}_{v_{1:w}} \left[\binom{n_1}{m} \left(\sum_{j=1}^w \omega_j \right)^m \left(1 - \sum_{j=1}^w \omega_j \right)^{n_1-m} \right] \\ &= \binom{n_1}{m} \mathbb{E}_{v_{1:w}} \left[\left(1 - \prod_{j=1}^w (1 - v_j) \right)^m \left(\prod_{j=1}^w (1 - v_j) \right)^{n_1-m} \right] \\ &= \binom{n_1}{m} \mathbb{E}_{v_{1:w}} \left[\sum_{l=0}^m (-1)^l \binom{m}{l} \prod_{j=1}^w (1 - v_j)^l \prod_{j=1}^w (1 - v_j)^{n_1-m} \right] \\ &= \binom{n_1}{m} \sum_{l=0}^m (-1)^l \binom{m}{l} \prod_{j=1}^w \mathbb{E}_{v_j} [(1 - v_j)^{l+n_1-m}] \\ &= \binom{n_1}{m} \sum_{l=0}^m (-1)^l \binom{m}{l} \left(\frac{\alpha}{\alpha + l + n_1 - m} \right)^w, \end{aligned} \quad (15)$$

and

$$\begin{aligned} \mathbb{E}_v [\mathbb{E}[K^{(w+1):\infty} | B = m, v]] &= \mathbb{E} [K^{(w+1):\infty} | B = m] \\ &= \sum_{i=1}^{n_2+n_1-m} \frac{\alpha}{\alpha + i - 1}, \end{aligned} \quad (16)$$

as, conditionally on $B = m$, $\mathbb{E}[K^{(w+1):\infty}]$ is the expected value of the number of distinct values in a sample of dimension $n_2 + n_1 - m$ distributed as a DP with concentration parameter α (see Pitman 2006). By combining (14), (15) and (16), we get

$$\begin{aligned} \mathbb{E}[K^{(w+1):\infty}] &= \sum_{m=0}^{n_1} \left(\sum_{i=1}^{n_2+n_1-m} \frac{\alpha}{\alpha+i-1} \right) \binom{n_1}{m} \sum_{l=0}^m (-1)^l \binom{m}{l} \left(\frac{\alpha}{\alpha+l+n_1-m} \right)^w \\ &= \sum_{m=0}^{n_1} \binom{n_1}{m} \left(\sum_{i=1}^{n_2+n_1-m} \frac{\alpha}{\alpha+i-1} \right) \sum_{l=0}^m (-1)^l \binom{m}{l} \left(\frac{\alpha}{\alpha+l+n_1-m} \right)^w. \end{aligned} \quad (17)$$

The proof is completed by replacing the expressions in (13) and (17) in (12). We observe that the result that we get does not depend on the assumption that $u_1 = 1$, which thus can be relaxed.

B Proofs of the results in Section 3

B.1 Proof of Proposition 4

We want to prove the full support of the thinned-DDP, where the full support is defined in the sense of Barrientos et al. (2012). In Theorem 1, they demonstrate that a sufficient condition to have full weak support is to ensure that the process assigns positive probability to product space of particular simplices. In the following, we show that such a condition holds for the thinned-DDP.

We study the setting where we only have two groups, but the proof can be easily generalized to any G . The sufficient condition of Barrientos et al. (2012) requires that

$$\mathbb{P}(|p_g(A_j) - q_{j,g}| < \epsilon, j = 1, \dots, k, g = 1, 2) = \mathbb{P}(\Omega_0) > 0, \quad (18)$$

where A_1, \dots, A_k is a measurable partition of Θ , and the $q_{j,g}$ are constants such that $q_{j,g} \geq 0$, $\sum_{j=1}^k q_{j,g} = 1$ for $g = 1, 2$.

Without loss of generality, we can assume that $P_0(A_j) > 0$ for $j = 1, \dots, k$, since if $P_0(A_j) = 0$ then $p_g(A_j) = 0$ a.s. and $q_{j,g} = 0$. We need to find a subset of Ω_0 with positive

probability. Assume that the sequences $\{\ell_{j,g}\}_{j \geq 1}$, $\{\theta_j\}_{j \geq 1}$ and $\{v_j\}_{j \geq 1}$ are independent.

Consider the set

$$\begin{aligned} \Omega_1 = \{ & \ell_{j,1} = 1 \text{ for } j = 1, \dots, k, \\ & \ell_{j,2} = 0 \text{ for } j = 1, \dots, k \text{ and } \ell_{j,2} = 1 \text{ for } j = k + 1, \dots, 2k\}, \end{aligned} \quad (19)$$

while $\ell_{j,1} \in \{0, 1\}$ for $j > k$, and $\ell_{j,2} \in \{0, 1\}$ for $j > 2k$, without restrictions. We assume that $\mathbb{P}(\Omega_1) > 0$ since this is true under all the considered prior distributions on the thinning variables.

Consider now

$$\Omega_2 = \{\omega : \theta_j \in A_j \text{ for } j = 1, \dots, k, \text{ and } \theta_{k+j} \in A_j \text{ for } j = 1, \dots, k\}. \quad (20)$$

Since $P_0(A_j) > 0$ for all j and the θ_j are independent, we have $\mathbb{P}(\Omega_2) > 0$.

Notice now that on Ω_1 we have

$$p_1(A) = \sum_{j=1}^{\infty} w_{j,1} \delta_{\theta_j}(A)$$

with

$$\begin{aligned} w_{j,1} &= v_j \prod_{h < j} (1 - v_h) \text{ for } j = 1, \dots, k \\ w_{j,1} &= v_j \ell_{j,1} \prod_{h < j} (1 - \ell_{h,1} v_h) \text{ for } j > k \end{aligned}$$

and

$$p_2(A) = \sum_{j=1}^{\infty} w_{j,2} \delta_{\theta_j}(A)$$

with

$$\begin{aligned} w_{j,2} &= 0 \text{ for } j = 1, \dots, k \\ w_{j,2} &= v_j \prod_{h=k+1}^{j-1} (1 - v_h) \text{ for } j = k + 1, \dots, 2k \\ w_{j,2} &= v_j \ell_{j,2} \prod_{h < j} (1 - \ell_{h,2} v_h) \text{ for } j > 2k. \end{aligned}$$

Thus, $(w_{1,1}, \dots, w_{k,1}) = \mathbf{w}_k$ and $(w_{k+1,2}, \dots, w_{2k,2}) = \mathbf{w}'_k$ are independent, given Ω_1 .

Consider now

$$\Omega_3 = \left\{ \omega : q_{j,1} - \frac{\epsilon}{k+1} < w_{j,1} < q_{j,1} + \frac{\epsilon}{k+1}, j = 1, \dots, k \right\} \quad (21)$$

and

$$S^k = \left\{ x_j \in \mathbb{R}^k : x_j > 0, \sum_{j=1}^k x_j < 1 \right\}.$$

Then, $\mathbb{P}(\Omega_3 \mid \Omega_1) = \mathbb{P}(\mathbf{w}_k \in B_3 \mid \Omega_1)$ where

$$B_3 = \left\{ \mathbf{y}_k \in S^k : q_{j,1} - \frac{\epsilon}{k+1} < y_{j,1} < q_{j,1} + \frac{\epsilon}{k+1}, j = 1, \dots, k \right\}.$$

B_3 is an open subset of S^k , at least for sufficiently small ϵ . On Ω_1 we have $\mathbf{w}_k = f(v_1, \dots, v_k)$, with $w_{1,1} = v_1$, $w_{j,1} = v_j \prod_{h < j} (1 - v_h)$: this mapping is one-to-one and continuous from $(0, 1)^k$ to S^k . It follows that $f^{-1}(B_3) = C_3$ is an open subset of $(0, 1)^k$.

Therefore,

$$\mathbb{P}(\Omega_3 \mid \Omega_1) = \mathbb{P}(\mathbf{w}_k \in B_3 \mid \Omega_1) = \mathbb{P}((v_1, \dots, v_k) \in C_3) > 0$$

since (v_1, \dots, v_k) has positive density (w.r.t. the Lebesgue measure) on $(0, 1)^k$.

A similar argument holds for \mathbf{w}'_k . Define

$$\Omega_4 = \left\{ \omega : q_{j,2} - \frac{\epsilon}{k+1} < w_{k+j,2} < q_{j,2} + \frac{\epsilon}{k+1}, j = 1, \dots, k \right\}. \quad (22)$$

Then, $\mathbb{P}(\Omega_4 \mid \Omega_1) = \mathbb{P}(\mathbf{w}'_k \in B_4 \mid \Omega_1)$ where

$$B_4 = \left\{ \mathbf{y}'_k \in S^k : q_{j,2} - \frac{\epsilon}{k+1} < y_{j,2} < q_{j,2} + \frac{\epsilon}{k+1}, j = 1, \dots, k \right\}.$$

On Ω_1 we have $\mathbf{w}'_k = f(v_{k+1}, \dots, v_{2k})$, with f as before. Therefore $f^{-1}(B_4) = C_4$ is an open subset of $(0, 1)^k$ and

$$\mathbb{P}(\Omega_4 \mid \Omega_1) = \mathbb{P}(\mathbf{w}'_k \in B_4 \mid \Omega_1) = \mathbb{P}((v_{k+1}, \dots, v_{2k}) \in C_4) > 0.$$

Furthermore,

$$\mathbb{P}(\Omega_1 \cap \Omega_3 \cap \Omega_4) = \mathbb{P}(\Omega_3, \Omega_4 \mid \Omega_1) \mathbb{P}(\Omega_1) = \mathbb{P}(\Omega_3 \mid \Omega_1) \mathbb{P}(\Omega_4 \mid \Omega_1) \mathbb{P}(\Omega_1)$$

since Ω_3 and Ω_4 are independent given Ω_1 .

Consider now $\Omega_5 = (\Omega_1 \cap \Omega_2 \cap \Omega_3 \cap \Omega_4)$:

$$\mathbb{P}(\Omega_5) = \mathbb{P}(\Omega_1 \cap \Omega_3 \cap \Omega_4) \mathbb{P}(\Omega_2) > 0$$

since $\{\theta_j\}$, $\{\ell_{j,g}\}$, and $\{v_j\}$ are independent.

Let us now show that $\Omega_5 \subseteq \Omega_0$, i.e., that conditions (19–22) imposed on $\{\theta_j\}$, $\{\ell_{j,g}\}$, and $\{v_j\}$ imply that $|p_g(A_j) - q_{j,g}| < \epsilon$, $j = 1, \dots, k$, $g = 1, 2$. This completes the proof since then $\mathbb{P}(\Omega_0) \geq \mathbb{P}(\Omega_5) > 0$.

Inequalities in Ω_3 imply that

$$q_{j,1} - \frac{\epsilon}{k+1} < w_{j,1}, \quad j = 1, \dots, k.$$

Summing w.r.t. j we get

$$1 - \frac{k}{k+1}\epsilon < \sum_{j=1}^k w_{j,1}$$

or,

$$\sum_{j=1}^k w_{j,1} < \epsilon \frac{k}{k+1}.$$

On Ω_5 we have, for $j = 1, \dots, k$

$$\begin{aligned} q_{j,1} - \frac{\epsilon}{k+1} < w_{j,1} \leq p_1(A_j) &\leq w_{j,1} + \sum_{h>k} w_{h,1} \\ &< q_{j,1} + \frac{\epsilon}{k+1} + \frac{\epsilon k}{k+1} = q_{j,1} + \epsilon \end{aligned}$$

since on Ω_5

$$p_1(A_j) = w_{j,1} + \sum_{h>k: \theta_h \in A_j} w_{h,1}.$$

Similarly, for p_2 , on Ω_5 we have, for $j = 1, \dots, k$

$$p_2(A_j) = w_{k+j,2} + \sum_{h>2k: \theta_h \in A_j} w_{h,2}.$$

As before, conditions in Ω_4 imply

$$1 - \epsilon \frac{k}{k+1} < \sum_{j=k+1}^{2k} w_{j,2}$$

and

$$\sum_{j>2k} w_{j,2} < \epsilon \frac{k}{k+1}.$$

Again on Ω_5 we have for $j = 1, \dots, k$

$$\begin{aligned} q_{j,2} - \frac{\epsilon}{k+1} &< w_{k+j,2} \leq p_2(A_j) \leq w_{k+j,2} + \sum_{h>2k} w_{h,2} \\ &< q_{j,2} + \frac{\epsilon}{k+1} + \frac{\epsilon k}{k+1} = q_{j,2} + \epsilon, \end{aligned}$$

therefore, $\Omega_5 \subseteq \Omega_0$ and the proof is completed.

B.2 Proof of Proposition 5

Suppose $\{\ell_{j,1}\}_{j \geq 1} \stackrel{\text{iid}}{\sim} \text{Bern}(p)$, $\{\ell_{j,2}\}_{j \geq 1} \stackrel{\text{iid}}{\sim} \text{Bern}(q)$, and that the sequences are independent.

The covariance (marginalizing w.r.t. $\ell_{1:2}$) is

$$\begin{aligned} \text{Cov}(p_1(A), p_2(A)) &= \mathbb{E}[(p_1(A) - \mathbb{E}[p_1(A)])(p_2(A) - \mathbb{E}[p_2(A)])] \\ &= \mathbb{E}[p_1(A)p_2(A)] - P_0(A)^2 \\ &= \mathbb{E}[\mathcal{E}_1] + \mathbb{E}[\mathcal{E}_2] + \mathbb{E}[\mathcal{E}_3] - P_0(A)^2 \end{aligned}$$

where

$$\begin{aligned} \mathcal{E}_1 &= \mathbb{E} \left[\sum_{h=1}^{\infty} \sum_{j=h+1}^{\infty} \ell_{h,1} \ell_{j,2} v_j v_h \prod_{i=1}^{j-1} (1 - \ell_{i,1} v_i) \prod_{k=1}^{h-1} (1 - \ell_{k,2} v_k) \delta_{\theta_j} \delta_{\theta_h} \right] \\ \mathcal{E}_2 &= \mathbb{E} \left[\sum_{h=1}^{\infty} \sum_{j=h+1}^{\infty} \ell_{h,2} \ell_{j,1} v_j v_h \prod_{i=1}^{j-1} (1 - \ell_{i,2} v_i) \prod_{k=1}^{h-1} (1 - \ell_{k,1} v_k) \delta_{\theta_j} \delta_{\theta_h} \right] \\ \mathcal{E}_3 &= \mathbb{E} \left[\sum_{j=1}^{\infty} \ell_{j,1} \ell_{j,2} v_j^2 \prod_{i=u_1}^{j-1} (1 - \ell_{i,1} v_i) \prod_{k=1}^{j-1} (1 - \ell_{k,2} v_k) \delta_{\theta_j} \right] \end{aligned}$$

$$\mathbb{E}[\mathcal{E}_1] = \mathbb{E} \left[\frac{P_0(A)^2}{(\alpha+1)^2(\alpha+2)} \sum_{j_1=1}^{\infty} \ell_{j_1,1} (\alpha + 2(1 - \ell_{j_1,2})) \prod_{i_1=1}^{j_1-1} \frac{\alpha}{\alpha + \ell_{i_1,1} + \ell_{i_1,2}} \sum_{j_2=j_1+1}^{\infty} \ell_{j_2,2} \prod_{i_2=j_1+1}^{j_2-1} \frac{\alpha}{\alpha + \ell_{i_2,2}} \right]$$

$$\begin{aligned}
&= \frac{P_0(A)^2}{(\alpha+1)^2(\alpha+2)} \sum_{j_1=1}^{\infty} p(\alpha+2(1-q)) \prod_{i_1=1}^{j_1-1} \frac{\alpha^2 + \alpha(3-p-q) + 2(1+pq-p-q)}{(\alpha+1)(\alpha+2)} \\
&\quad \times \sum_{j_2=j_1+1}^{\infty} q \prod_{i_2=j_1+1}^{j_2-1} \frac{\alpha+1-q}{\alpha+1} \\
&= \frac{P_0(A)^2 pq(\alpha+2(1-q))}{(\alpha+1)^2(\alpha+2)} \sum_{j_1=1}^{\infty} \left(\frac{\alpha^2 + \alpha(3-p-q) + 2(1+pq-p-q)}{(\alpha+1)(\alpha+2)} \right)^{j_1-1} \sum_{j_2=j_1+1}^{\infty} \left(\frac{\alpha+1-q}{\alpha+1} \right)^{j_2-j_1-1} \\
&= P_0(A)^2 \frac{p(\alpha+2-2q)}{\alpha(p+q) + 2(p+q-pq)}
\end{aligned}$$

Similarly, $\mathbb{E}[\mathcal{E}_2] = P_0(A)^2 \frac{q(\alpha+2-2p)}{\alpha(p+q) + 2(p+q-pq)}$.

$$\begin{aligned}
\mathbb{E}[\mathcal{E}_3] &= \mathbb{E} \left[\frac{2P_0(A)}{(\alpha+1)(\alpha+2)} \sum_{j=1}^{\infty} \ell_{j,1} \ell_{j,2} \prod_{i=1}^{j-1} \frac{\alpha}{\alpha + \ell_{i,1} + \ell_{i,2}} \right] \\
&= \frac{2P_0(A)}{(\alpha+1)(\alpha+2)} pq \sum_{j=1}^{\infty} \left(\frac{\alpha^2 + \alpha(3-p-q) + 2(1+pq-p-q)}{(\alpha+1)(\alpha+2)} \right)^{j-1} \\
&= \frac{2pq P_0(A)}{\alpha(p+q) + 2(p+q-pq)}
\end{aligned}$$

Hence,

$$\begin{aligned}
\text{Cov}(p_1(A), p_2(A)) &= \frac{P_0(A)^2 [p(\alpha+2-2q) + q(\alpha+2-2p)]}{\alpha(p+q) + 2(p+q-pq)} + \frac{2pq P_0(A)}{\alpha(p+q) + 2(p+q-pq)} - P_0(A)^2 \\
&= \frac{-2pq P_0(A)^2}{\alpha(p+q) + 2(p+q-pq)} + \frac{2pq P_0(A)}{\alpha(p+q) + 2(p+q-pq)} \\
&= \frac{2pq}{\alpha(p+q) + 2(p+q-pq)} P_0(A) (1 - P_0(A))
\end{aligned}$$

Finally, the correlation is obtained as

$$\text{Corr}(p_1(A), p_2(A)) = \frac{2pq(\alpha+1)}{\alpha(p+q) + 2(p+q-pq)}$$

B.3 Proof of Proposition 6

Consider again Equation (5) from Franzolini et al. (2025). The marginal probability of ties can be obtained by marginalizing u_1 and u_2 as

$$\Pr(y_{i,1} = y_{k,2}) = \mathbb{E}_{u_1, u_2} [\Pr(y_{i,1} = y_{k,2} \mid u_1, u_2)]$$

$$\begin{aligned}
&\stackrel{(a)}{=} \mathbb{E}_{u_1, u_2} \left[\text{Corr}(p_1(A), p_2(A) \mid u_1, u_2) \sqrt{\text{Pr}(y_{i,1} = y_{i',1} \mid u_1, u_2) \text{Pr}(y_{k,2} = y_{k',2} \mid u_1, u_2)} \right] \\
&\stackrel{(b)}{=} \mathbb{E}_{u_1, u_2} \left[\text{Corr}(p_1(A), p_2(A) \mid u_1, u_2) \sqrt{\text{Pr}(y_{i,1} = y_{i',1}) \text{Pr}(y_{k,2} = y_{k',2})} \right] \\
&= \mathbb{E}_{u_1, u_2} [\text{Corr}(p_1(A), p_2(A) \mid u_1, u_2)] \sqrt{\text{Pr}(y_{i,1} = y_{i',1}) \text{Pr}(y_{k,2} = y_{k',2})},
\end{aligned}$$

where (a) follows the application of Eq. (5) to the multivariate species sampling process conditioned on (u_1, u_2) , and (b) follows the fact that the probability of ties within each distribution does not depend on the specific values of u_1 and u_2 . Hence,

$$\begin{aligned}
\text{Corr}(p_1(A), p_2(A)) &= \frac{\mathbb{E}_{u_1, u_2} [\text{Corr}(p_1(A), p_2(A) \mid u_1, u_2)] \sqrt{\text{Pr}(y_{i,1} = y_{i',1}) \text{Pr}(y_{k,2} = y_{k',2})}}{\sqrt{\text{Pr}(y_{i,1} = y_{i',1}) \text{Pr}(y_{k,2} = y_{k',2})}} \\
&= \mathbb{E}_{u_1, u_2} [\text{Corr}(p_1(A), p_2(A) \mid u_1, u_2)].
\end{aligned}$$

Consider the result of Corollary 1. If $(u_1 - 1)$ and $(u_2 - 1)$ have independent Poisson distributions with parameters λ_1 and λ_2 , then $u_2 - u_1$ has a Skellam distribution and

$$\text{Corr}(p_1(A), p_2(A)) = e^{-\lambda_1 - \lambda_2} \left(I_0(2\sqrt{\lambda_1 \lambda_2}) + \sum_{k=1}^{\infty} \left(\frac{\alpha}{1 + \alpha} \right)^k \left[\left(\frac{\lambda_1}{\lambda_2} \right)^{k/2} + \left(\frac{\lambda_2}{\lambda_1} \right)^{k/2} \right] I_k(2\sqrt{\lambda_1 \lambda_2}) \right)$$

If $|u_2 - u_1| \sim \text{Poisson}(\lambda)$, we compute the marginal correlation starting from the conditional one. Denote $|u_2 - u_1| = x$, then

$$\begin{aligned}
\text{Corr}(p_1, p_2) &= \mathbb{E}_x \left[\left(\frac{\alpha}{\alpha + 1} \right)^x \right] \\
&= \sum_{x=0}^{\infty} \left(\frac{\alpha}{\alpha + 1} \right)^x e^{-\lambda} \frac{\lambda^x}{x!} \\
&= e^{-\lambda} \sum_{x=0}^{\infty} \left(\frac{\alpha \lambda}{\alpha + 1} \right)^x \frac{1}{x!} e^{-\frac{\alpha \lambda}{\alpha + 1}} e^{\frac{\alpha \lambda}{\alpha + 1}} \\
&= \exp \left\{ -\lambda + \frac{\alpha \lambda}{\alpha + 1} \right\} = \exp \left\{ \frac{-\alpha \lambda - \lambda + \alpha \lambda}{\alpha + 1} \right\} = \exp \left\{ \frac{-\lambda}{\alpha + 1} \right\}.
\end{aligned}$$

C Other prior distributions for the thinning variables

In this Section, we outline two additional prior distributions for the thinning sequences that ensure full weak support of the model while allowing more refined specifications of the dependence between random measures.

C.1 Dependent-Bernoulli thinning

The prior specification in Section 3.1 assumed independent Bernoulli random variables $\ell_{j,g} \sim \text{Bern}(\pi_g)$ for all group g and index j . With this prior, we are only modeling the *marginal* probability of observing atom j in distribution p_g , regardless of the presence or absence of the atom in the other distributions. A more refined specification could instead explicitly model this dependence.

Consider, for simplicity, two distributions p_1 and p_2 . We introduce a dependent prior for $\ell_{1,2}$. Specifically, for all $j \geq 1$, we model the couple $(\ell_{j,1}, \ell_{j,2})$ as dependent Bernoulli random variables with probabilities:

$$\left\{ \begin{array}{l} \pi_{11} = \Pr(\ell_{j,1} = \ell_{j,2} = 1) \\ \pi_{01} = \Pr(\ell_{j,1} = 0, \ell_{j,2} = 1) \\ \pi_{10} = \Pr(\ell_{j,1} = 1, \ell_{j,2} = 0) \\ \pi_{00} = \Pr(\ell_{j,1} = \ell_{j,2} = 0) \end{array} \right.$$

under the constraint that $\pi_{11} + \pi_{00} + \pi_{01} + \pi_{10} = 1$. The couples are still independent for different $j \geq 1$.

Similar to the other prior specifications, it is possible to compute the marginal correlation between p_1 and p_2 , marginalizing the sequences $\ell_{1,2}$. The marginal correlation is then obtained as

$$\text{Corr}(p_1, p_2) = \frac{2\pi_{11}(\alpha + 1)}{(\alpha + 2)(1 - \pi_{00}) + \alpha\pi_{11}}$$

An alternative parameterization allows modeling, instead of all the joint probabilities, the marginal probabilities and the correlations between all couples. With this parameterization, it is intuitive how to extend the framework to more than two groups.

C.2 Symmetric eventually single-atom thinning

The eventually single-atom formulation defined in Section 2.1 implies a nested structure between distributions. However, it is straightforward to relax the constraint by defining a symmetric counterpart. Consider, for simplicity, the case with two distributions. We define a blocked structure for the thinning sequences, so that a set of distribution-specific atoms characterizes each random measure. For example, one could define the following block structure:

- $\ell_{j,1} = 1$ and $\ell_{j,2} = 1$ for $j = 1, \dots, b_0$,
- $\ell_{j,1} = 1$ and $\ell_{j,2} = 0$ for $j = b_0 + 1, \dots, b_0 + b_1$,
- $\ell_{j,1} = 0$ and $\ell_{j,2} = 1$ for $j = b_0 + b_1 + 1, \dots, b_0 + b_1 + b_2$,
- $\ell_{j,1} = 1$ and $\ell_{j,2} = 1$ for $j \geq b_0 + b_1 + b_2 + 1$.

Hence, the distributions share the first b_0 atoms; the following b_1 atoms are specific to p_1 ; then, b_2 are specific to p_2 ; and, finally, all remaining atoms are common:

$$p_1(\cdot) = \sum_{j=1}^{b_0+b_1} \left[v_j \prod_{h=1}^{j-1} (1-v_h) \right] \delta_{\theta_j}(\cdot) + \left\{ \prod_{h=1}^{b_0+b_1} (1-v_h) \right\} \sum_{j=b_0+b_1+b_2+1}^{\infty} \left[v_j \prod_{h=b_0+b_1+b_2+1}^{j-1} (1-v_h) \right] \delta_{\theta_j}(\cdot),$$

$$p_2(\cdot) = \sum_{j=1}^{b_0} \left[v_j \prod_{h=1}^{j-1} (1-v_h) \right] \delta_{\theta_j}(\cdot) + \left\{ \prod_{h=1}^{b_0} (1-v_h) \right\} \sum_{j=b_0+b_1+1}^{\infty} \left[v_j \prod_{h=b_0+b_1+1}^{j-1} (1-v_h) \right] \delta_{\theta_j}(\cdot)$$

This formulation can be extended to any number of groups G by assuming that, for $j = b_0 + b_1 + \dots + b_{g-1} + 1, \dots, b_0 + b_1 + \dots + b_g$, $\ell_{j,g}$ is equal to one for distribution g and zero for the others.

The analytical tractability of the eventually single-atom structure is preserved in this symmetric version, as evidenced by the simple form of the correlation between the distributions p_1 and p_2 :

$$\text{Corr}(p_1(A), p_2(A); b_{0:2}) = 1 - \left(\frac{\alpha}{\alpha + 2} \right)^{b_0} \left[1 - \left(\frac{\alpha}{\alpha + 1} \right)^{b_1+b_2} \right].$$

The correlation depends on the sequences of thinning variables solely through the number of initial shared atoms b_0 and the sum of b_1 and b_2 , which represents the total number of atoms not shared by p_1 and p_2 . Indeed, when $b_1 = b_2 = 0$, the correlation equals one, as $p_1 = p_2$.

C.2.1 Symmetric eventually single-atom Poisson thinning

One can assign independent Poisson prior distributions to all parameters modeling the length of each block, $b_r \sim \text{Pois}(\lambda_r)$ for $r = 0, 1, 2$. Then, the marginal correlation is obtained as

$$\text{Corr}(p_1, p_2) = 1 - \exp\left\{-\frac{2\lambda_0}{\alpha + 2}\right\} \left[1 - \exp\left\{-\frac{\lambda_1 + \lambda_2}{\alpha + 1}\right\}\right].$$

If $\lambda_1 = \lambda_2 = 0$, there are no distribution-specific atoms, and the correlation is one.

D Correlations with parent process

We consider a vector $p_{1:G}$ of thinned-DDPs obtained by thinning a common Dirichlet process p (see Definition 1), here referred to as the “parent process”. Focusing without loss of generality on the first component p_1 , we study its correlation with the parent process p . The results below are direct specializations of those in Sections 2 and 3, obtained by replacing p_2 with p , which corresponds to setting ℓ_2 as an infinite sequence of ones.

A direct application of Proposition 1 leads to the following corollary.

Corollary D.1. If $p_1 \sim \text{thinned-DDP}(\alpha, P_0, \ell_1)$, with parent process p , then, for any $A \in \mathcal{B}$, the correlation between $p_1(A)$ and $p(A)$ is given by

$$\begin{aligned} \text{Corr}(p_1(A), p(A); \ell_1) &= \frac{2}{(\alpha + 2)} \sum_{j \geq 1} \ell_{j,1} \prod_{h < j} \frac{\alpha}{\alpha + \ell_{h,1} + 1} \\ &= \frac{2}{(\alpha + 2)} \sum_{j \geq 1} \ell_{j,1} \alpha^{j-1} \left(\frac{1}{\alpha + 2}\right)^{\sum_{h=1}^{j-1} \ell_{h,1}} \left(\frac{1}{\alpha + 1}\right)^{\sum_{h=1}^{j-1} (1 - \ell_{h,1})}. \end{aligned}$$

A direct application of Corollary 1 leads to the following corollary.

Corollary D.2. If $p_1 \sim \text{thinned-DDP}(\alpha, P_0, u_1)$ with parent process p , then, for any $A \in \mathcal{B}$, the correlation between $p_1(A)$ and $p(A)$ is given by

$$\text{Corr}(p_1(A), p(A); u_1) = \left(\frac{\alpha}{\alpha + 1} \right)^{u_1 - 1}.$$

A direct application of Proposition 5 leads to the following corollary.

Corollary D.3. Let $p_1 \sim \text{thinned-DDP}(\alpha, P_0, \ell_1)$ with parent process p , and consider a measurable set $A \in \mathcal{B}$. Assume $\ell_{j,1} \stackrel{\text{iid}}{\sim} \text{Bern}(\pi_1)$, for $j \geq 1$. The correlation between $p_1(A)$ and $p(A)$ is

$$\text{Corr}(p_1(A), p(A)) = \frac{2\pi_1(\alpha + 1)}{\alpha(\pi_1 + 1) + 2}.$$

A direct application of Proposition 6 leads to the following corollary.

Corollary D.4. Let $p_1 \sim \text{thinned-DDP}(\alpha, P_0, u_1)$ with parent process p , and consider a measurable set $A \in \mathcal{B}$. Assume $u_1 - 1 \stackrel{\text{iid}}{\sim} \text{Poisson}(\lambda_1)$. The correlation between $p_1(A)$ and $p(A)$ is

$$\text{Corr}(p_1(A), p(A)) = \exp \left\{ -\frac{\lambda_1}{\alpha + 1} \right\}.$$

E Blocked Gibbs sampler

Consider the Gaussian mixture model of Section 4. Before detailing the algorithm, it is useful to introduce a hierarchical representation of the model based on the cluster allocation variables $z_{i,g} \in \{1, 2, \dots\}$. These variables have a discrete distribution $\Pr(z_{i,g} = k \mid \{\omega_{j,g}\}_{j \geq 1}) = \omega_{k,g}$, for $k \geq 1$, and they are such that $f(y_{i,g} \mid z_{i,g} = k, \{\mu_j, \sigma_j^2\}_{j \geq 1}) = \phi(y_{i,g} \mid \mu_k, \sigma_k^2)$. With this model representation, the blocked Gibbs sampler proceeds by iteratively updating each parameter from its full conditional distribution, as follows

1. Update the thinning variables $\{\ell_{j,g}\}_{j=0}^T$, $g = 1, \dots, G$.

Assume that the last occupied cluster is $K = \max\{j : n_{j,g} > 0, g = 1, \dots, G\}$, where $n_{j,g}$ is the number of observations of group g allocated to cluster j , for $g = 1, \dots, G$ and $j \geq 1$.

For $k = K, K - 1, \dots, 1$, and for $g = 1, \dots, G$, update the thinning variable $\ell_{k,g}$:

$$\ell_{k,g} \mid \dots \sim \begin{cases} \delta_1 & \text{if } n_{k,g} > 0 \\ \text{Bernoulli}(\pi^*) & \text{if } n_{k,g} = 0 \end{cases}$$

with

$$\pi^* = D^{-1}(1 - v_k)^{\sum_{h=k+1}^K n_{h,g}} \pi_g$$

and $D = (1 - v_k)^{\sum_{h=k+1}^K n_{h,g}} \pi_g + 1 - \pi_g$.

Sample a new thinning variable from the prior, $\ell_{k,g} \sim \text{Bernoulli}(\pi_g)$, for $k = K + 1, K + 2, \dots, T$, where T is the truncation level.

2. Update the beta random variables $\{v_j\}_{j=1}^\infty$. For $k = 1, 2, \dots, T$

$$v_k \mid \dots \sim \text{Beta} \left(1 + \sum_{g=1}^G n_{k,g}, \alpha + \sum_{g=1}^G \left\{ \ell_{k,g} \left(\sum_{h=k+1}^K n_{h,g} \right) \right\} \right).$$

With the updated variables, compute the weights via a thinned-stick-breaking process.

3. Update the cluster allocation $z_{i,g}$.

For $g = 1, \dots, G$ and $i = 1, \dots, N_g$, sample $z_{i,g}$ from a multinomial distribution

$$\Pr(z_{i,g} = k \mid \dots) = \begin{cases} \phi(y_{i,g} \mid \mu_k, \sigma_k^2) \left[v_k \prod_{h=1}^{j-1} (1 - \ell_{h,g} v_h) \right] & \text{if } \ell_{k,g} = 1 \\ 0 & \text{if } \ell_{k,g} = 0 \end{cases}$$

for $k = 1, \dots, T$.

4. Sample the kernel parameters $\{\mu_k, \sigma_k^2\}_{k=1}^\infty$.

For $k = 1, 2, \dots, T$, denote with A_k the set $A_k = \{(g, i) : z_{i,g} = k\}$ and with n_k its cardinality, $n_k = \sum_{g=1}^G \sum_{i=1}^{N_g} \mathbb{I}(z_{i,g} = k)$, sample

$$(1/\sigma_k^2 \mid \dots) \sim \text{Gamma} \left(\gamma_0 + \frac{n_k}{2}, \lambda_0 + \frac{1}{2} \left\{ \sum_{A_k} (y_{i,g} - \bar{y}_{A_k})^2 + \frac{\tau_0 n_k}{\tau_0 + n_k} (\bar{y}_{A_k} - \mu_0)^2 \right\} \right)$$

$$(\mu_k \mid \sigma_k^2, \dots) \sim \text{N} \left(\frac{\tau_0 \mu_0 + \sum_{A_k} y_{i,g}}{\tau_0 + n_k}, \frac{\sigma_k^2}{\tau_0 + n_k} \right)$$

where $\bar{y}_{A_k} = n_k^{-1} \sum_{A_k} y_{i,g}$.

5. Update the distribution-specific thinning probabilities π_g .

For $g = 1, \dots, G$, sample a new value from a beta distribution with updated parameters,

$$\pi_g \mid \dots \sim \text{Beta} \left(a_\pi + \sum_{j=1}^T \ell_{j,g}, b_\pi + T - \sum_{j=1}^T \ell_{j,g} \right).$$

F Additional details on the simulation studies

Estimation of the thinned-DDP was performed using the Gibbs sampler outlined in Section 4; for the complete-pooling and no-pooling models, we used a standard blocked Gibbs sampler for DP mixtures. The truncation parameter was set to 100 for all models. Posterior inference for the CAM and the GM-DDP was performed using the R packages SANple (D’Angelo & Denti 2023) and BNPmix (Corradin et al. 2021), respectively. We ran all algorithms for 3,000 iterations, discarding the first 2,000 as burn-in. Figure F1 shows the distribution of the computation time (in logarithmic scale) for the thinned-DDP, the CAM, and the GM-DDP.

The concentration parameter α for the thinned-DDP, the complete-pooling and no-pooling mixtures, and the GM-DDP was fixed to 1, while it is random for the CAM. The thinning probabilities π_g , for $g = 1, \dots, G$, in the thinned-DDP were random and assigned

a Beta(3, 3) prior distribution. The parameters of the normal-inverse gamma base measure were fixed to $(\mu_0 = \bar{y}, \tau_0 = 0.01, \gamma_0 = 2.5, \lambda_0 = 1.5)$.

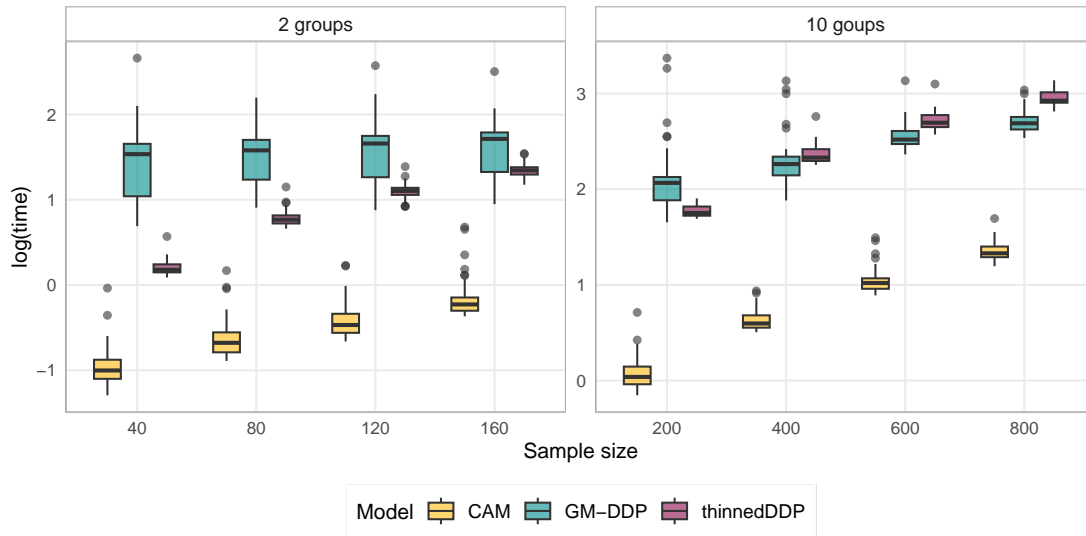


Figure F1: Distribution of the computational time for the thinned-DDP, the CAM, and the GM-DDP mixture on the simulated data.

F.1 Additional figures

Figure F2 displays a summary of the distribution of the average length of the pointwise 95% highest posterior density (HPD) credible intervals for the thinned-DDP, the complete pooling, and no pooling mixtures. Figure F3 displays the same quantity for the thinned-DDP, the GM-DDP, and the CAM.

Finally, we report additional graphs with the posterior point estimates of the densities and the credible bands for the thinned-DDP, the CAM, and the GM-DDP. Specifically, we show an example with $G = 2$ and $G = 10$ and the smallest sample size (Figures F4, F5, and F6); and with $G = 2$ and $G = 10$, for the largest sample size (Figures F7, F8 and F9).

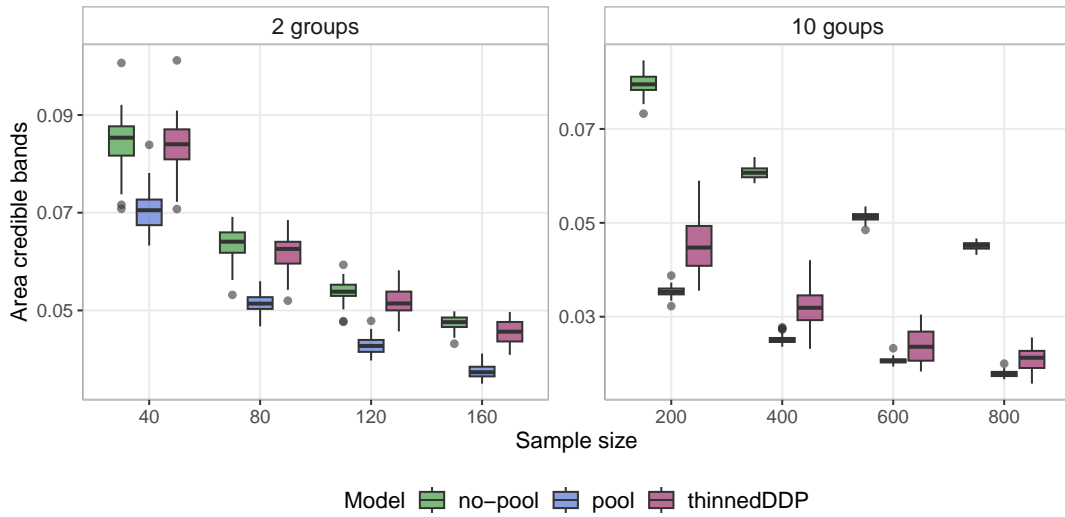


Figure F2: Distribution of the average pointwise size of the credible bands for the thinned-DDP, the complete-pooling, and the no-pooling DP mixture on the simulated data.

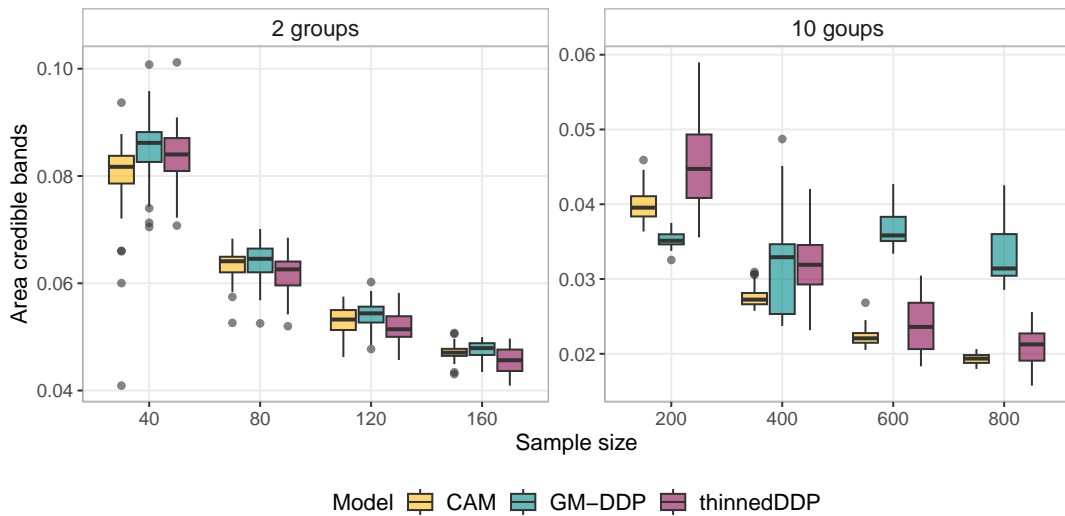


Figure F3: Distribution of the average pointwise size of the credible bands for the thinned-DDP, the CAM, and the GM-DDP mixture on the simulated data.

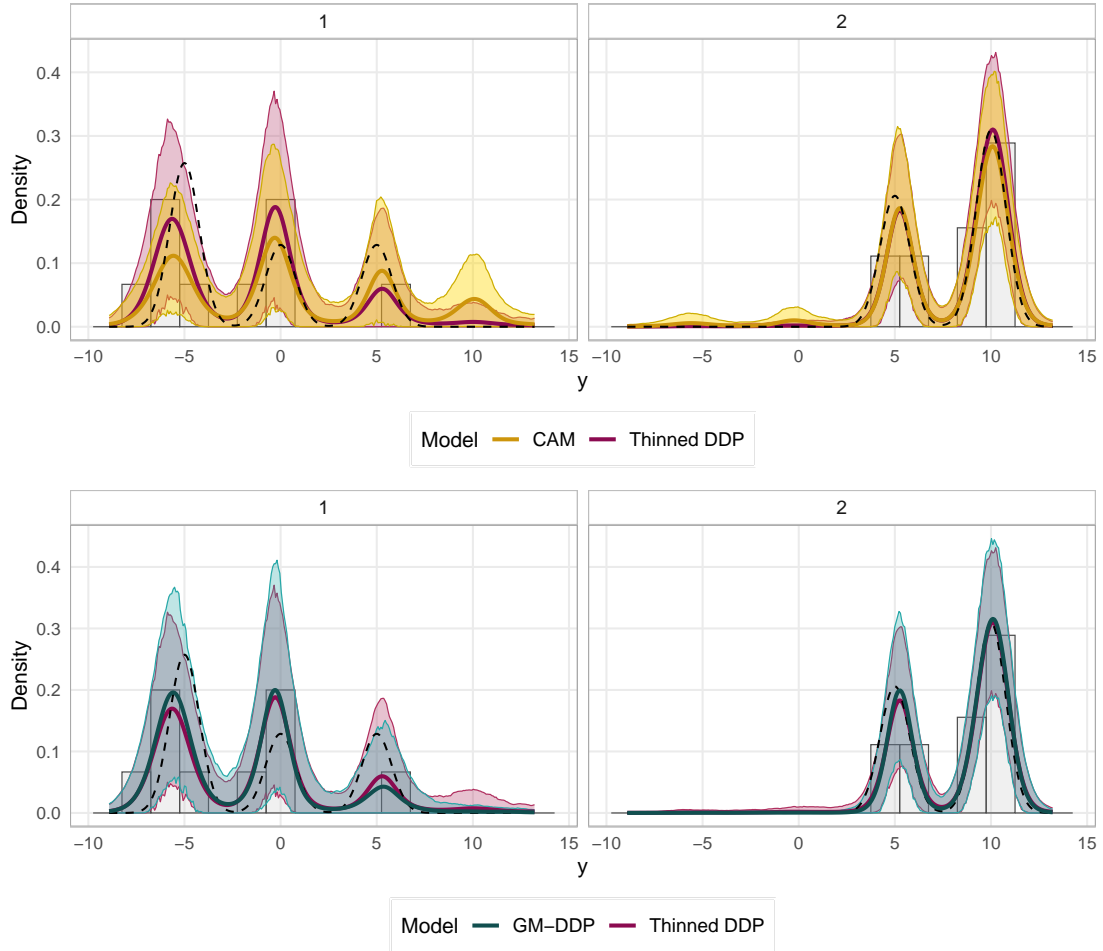


Figure F4: $G = 2$, $N = 40$: histogram of the data, posterior density estimates (continuous lines), and credible bands (shaded areas). The black dashed line represents the true data-generating density. Top panels: estimates of the thinned-DDP and the CAM; bottom panels: estimates of the thinned-DDP and the GM-DDP.

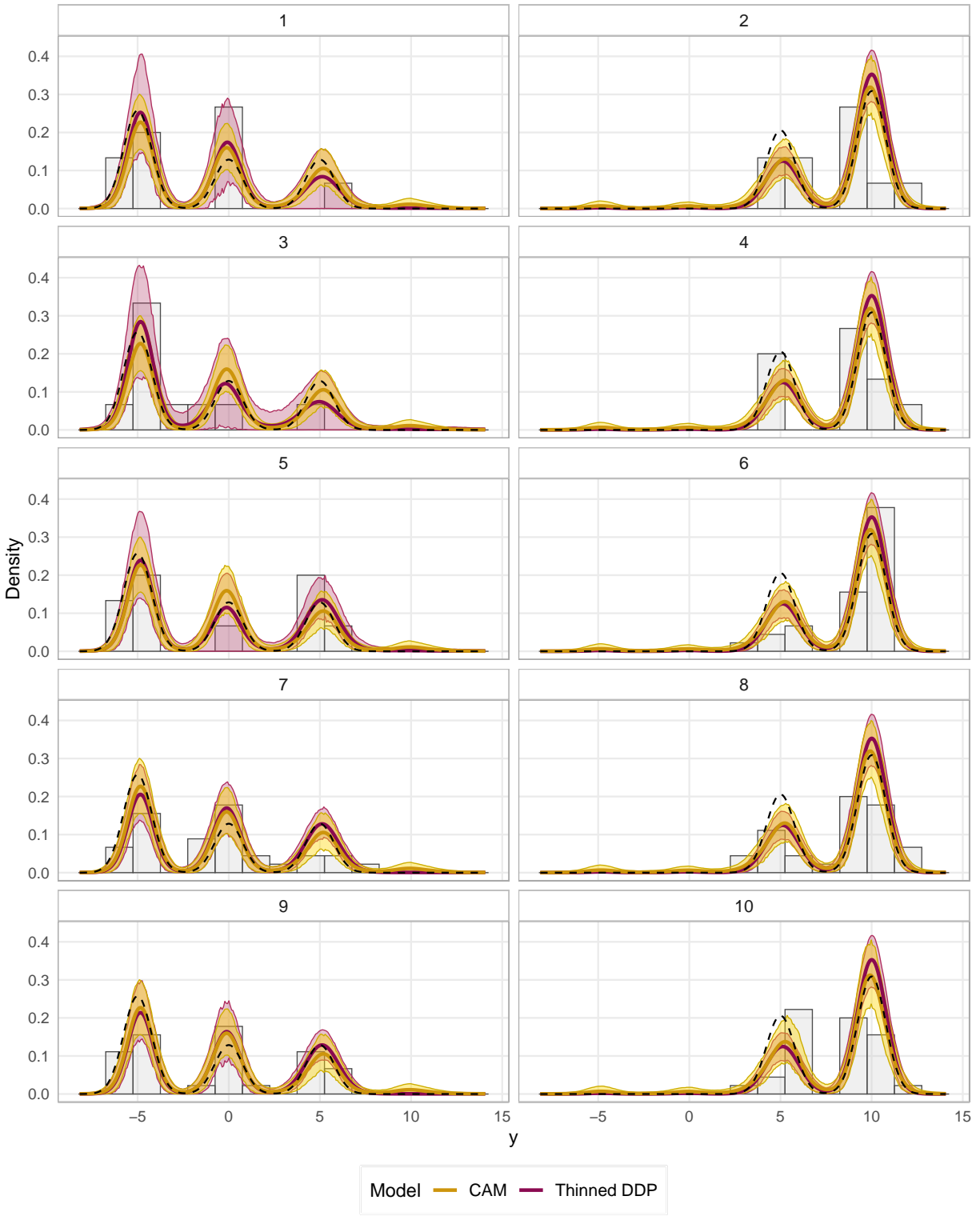


Figure F5: $G = 10$, $N = 200$: histogram of the data, posterior density estimates (continuous lines), and credible bands (shaded areas). The black dashed line represents the true data-generating density. Estimates of the thinned-DDP and the CAM

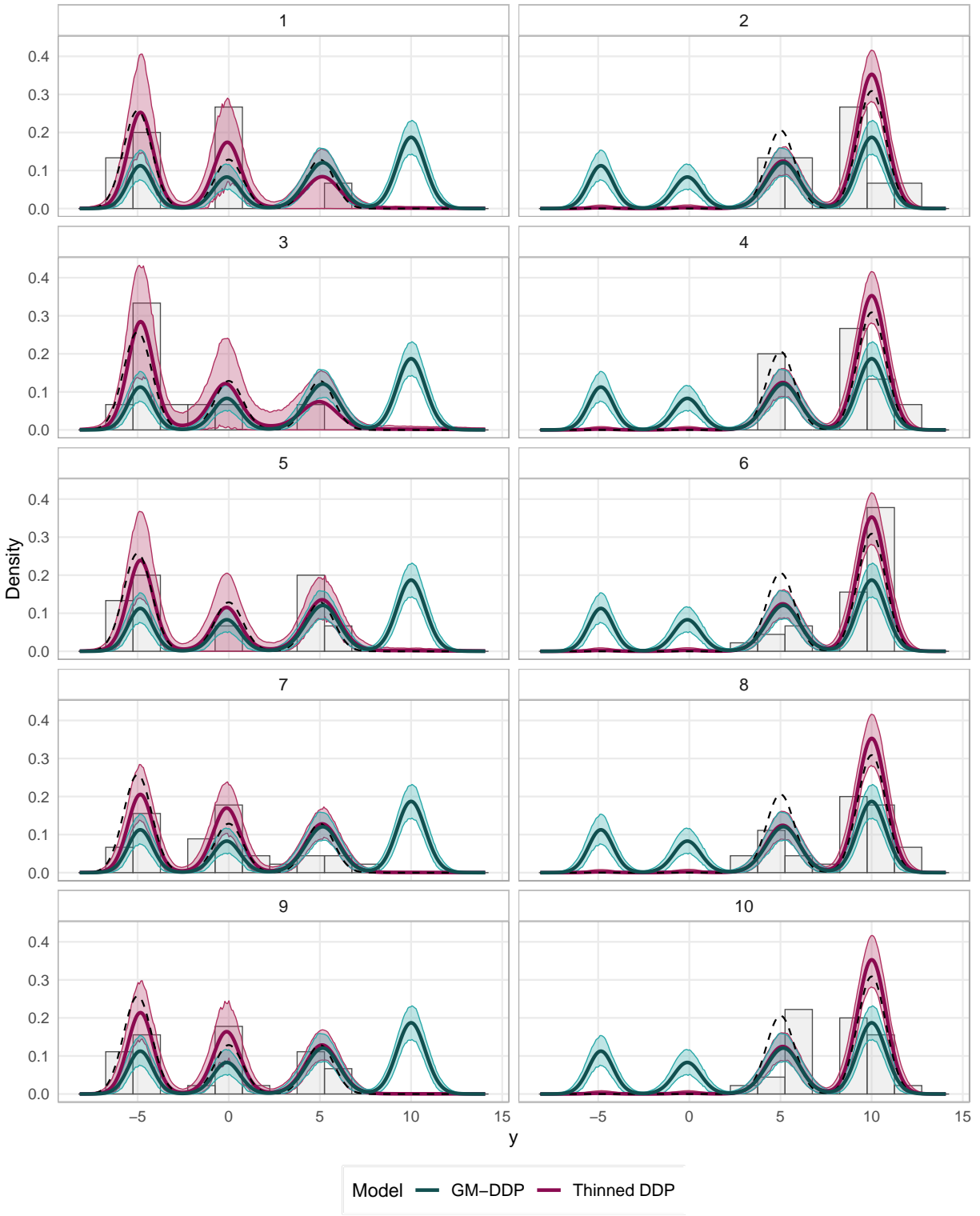


Figure F6: $G = 10$, $N = 200$: histogram of the data, posterior density estimates (continuous lines), and credible bands (shaded areas). The black dashed line represents the true data-generating density. Estimates of the thinned-DDP and the GM-DDP.

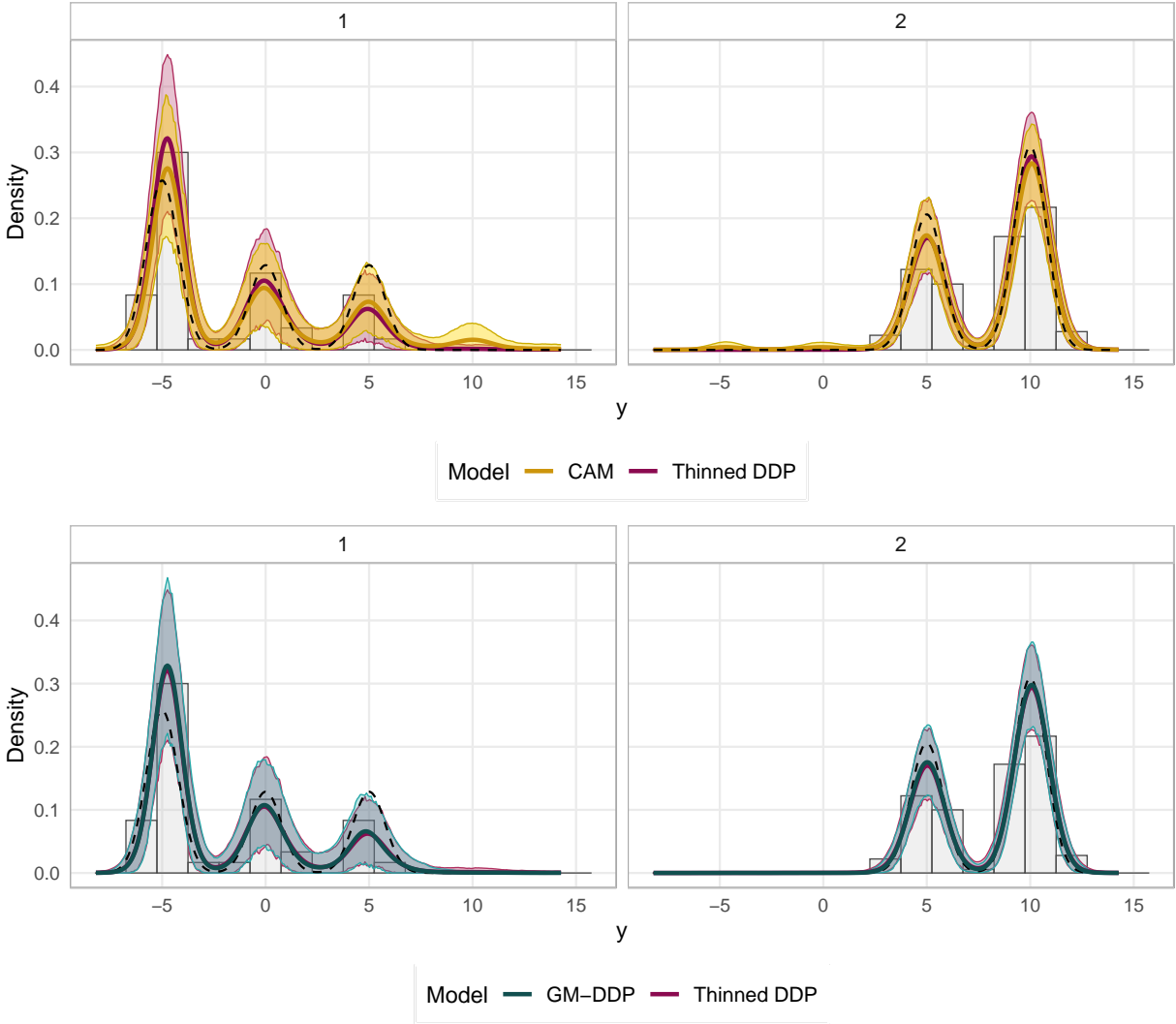


Figure F7: $G = 2$, $N = 160$: histogram of the data, posterior density estimates (continuous lines), and credible bands (shaded areas). The black dashed line represents the true data-generating density. Top panels: estimates of the thinned-DDP and the CAM; bottom panels: estimates of the thinned-DDP and the GM-DDP.

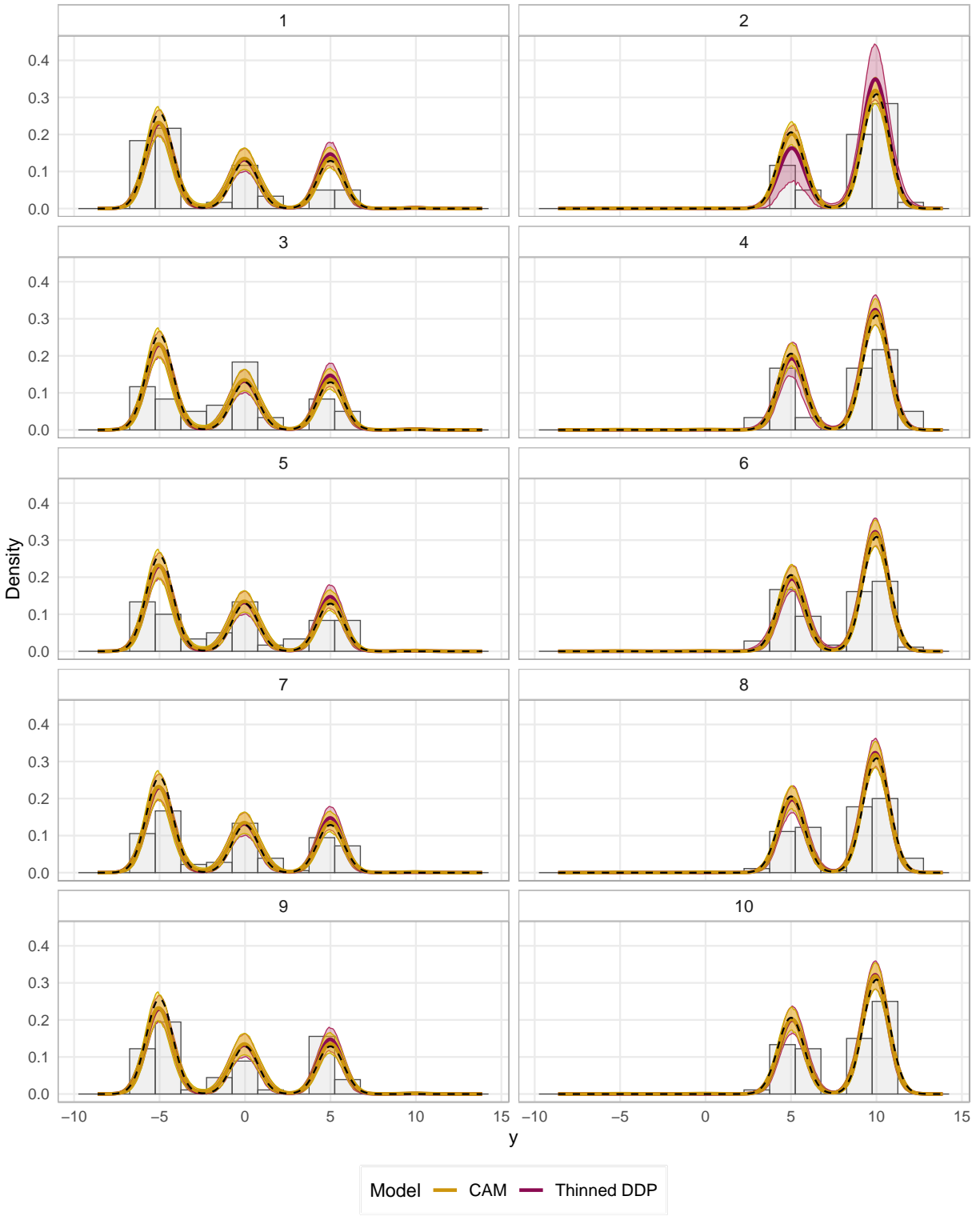


Figure F8: $G = 10$, $N = 800$: histogram of the data, posterior density estimates (continuous lines), and credible bands (shaded areas). The black dashed line represents the true data-generating density. Estimates of the thinned-DDP and the CAM

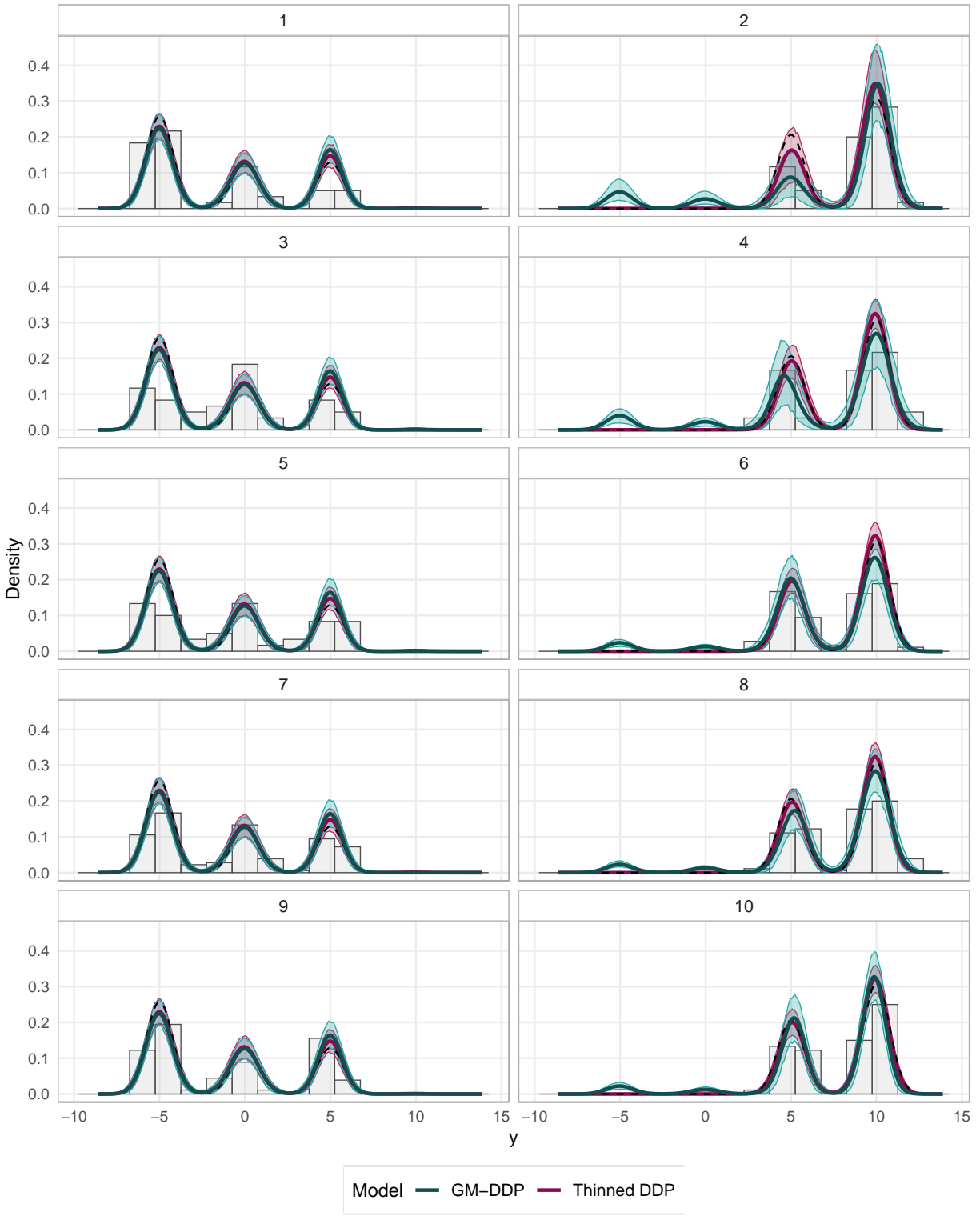


Figure F9: $G = 10$, $N = 800$: histogram of the data, posterior density estimates (continuous lines), and credible bands (shaded areas). The black dashed line represents the true data-generating density. Estimates of the thinned-DDP and the GM-DDP.

G Additional details on the real data analysis

Figure G10 shows the boxplots of the distribution of the gestational age in the 12 hospitals.

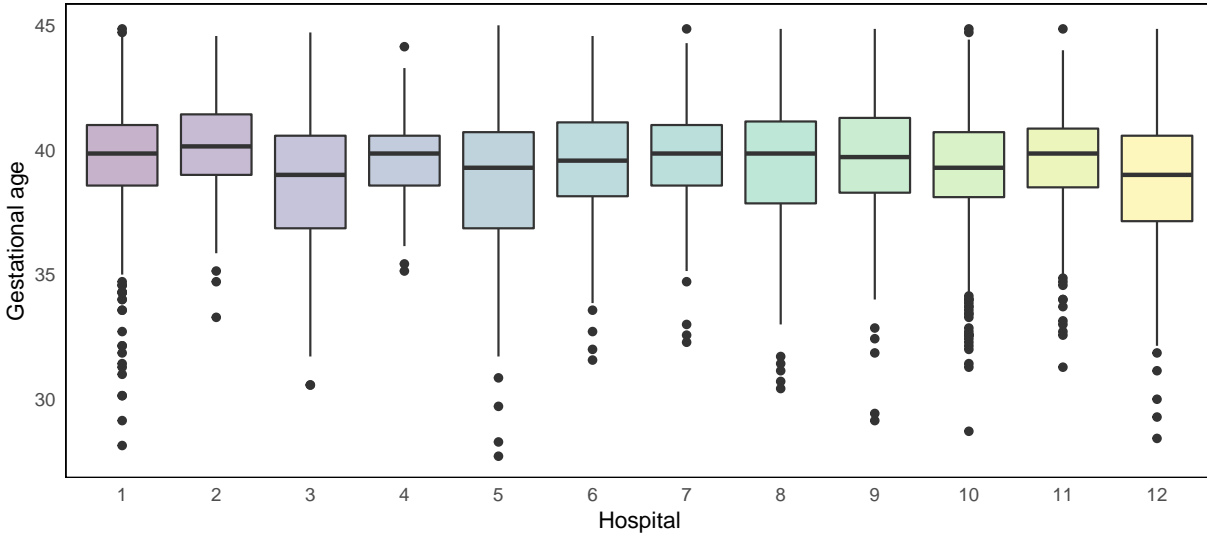


Figure G10: Distribution of the gestational age in the 12 centers.

Figure G11 shows the estimated total variation distance computed on the group-specific densities between all pairs of hospitals.

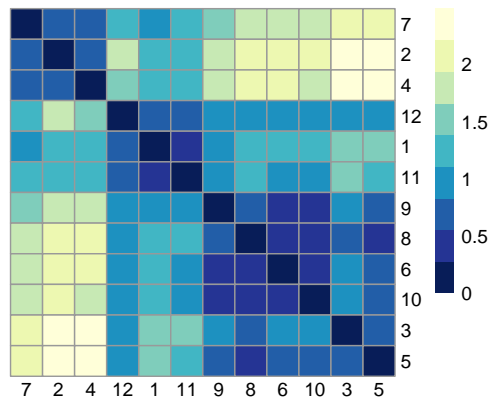


Figure G11: Heatmap of the pairwise TV distance between couples of hospitals.